Downscaling Global Climate Model Data with CHELSA

Dr. Abby Lute (alute@woodwellclimate.org)
December 2022. *Updated March, 2023*

Abstract

High resolution (~1 km) projections of future climate are needed to inform local to regional risk assessments and adaptation plans. One way to achieve this level of spatial resolution is to downscale global climate model outputs. The CHELSA downscaling approach is one such approach to downscale climatologies of temperature (mean, min, and max) and precipitation to 1 km globally. Here we describe the CHELSA downscaling approach, modifications to the downscaling code to better fit the purposes of the Woodwell Risk Team, and the development of downscaled datasets from CMIP6 based on the modified code. Currently the downscaled datasets include 1 km resolution global representations of mean, min, and max temperature and precipitation monthly climatologies for 17 models, 2 scenarios (SSP245 and SSP585), and three warming levels (1°C, 1.5°C, and 2°C). We present an evaluation of the downscaled data relative to raw CMIP6 data, to Daymet, and to published outputs from the original CHELSA downscaling approach. The modified code is available at https://github.com/WoodwellRisk/CHELSA_downscaling and the downscaled outputs are available upon request from the Woodwell Risk Team.

1. Introduction

Global Climate Model (GCM) outputs, such as those from CMIP6, typically provide climate data at spatial resolutions of 1° to 2°. While this is impressive compared to the spatial resolutions employed just a decade or two ago, it is still of limited utility for local and regional climate impact assessments. Downscaling, sometimes combined with bias-correction, is often used to enhance the spatial resolution of GCM outputs. Downscaling approaches include statistical methods spanning interpolation to more complex approaches and dynamical methods which use regional climate models to re-simulate the climate in a given sub domain. Due to their relative simplicity and lower computational cost, statistical downscaling approaches are more often employed when global coverage is required, the turnaround time is short, or computational and scientific resources are not available for a more expensive approach.

One simple statistical downscaling approach is based on the climatologies at high resolution for the earth's land surface areas (CHELSA) dataset, hereafter referred to as the CHELSA method (https://pypi.org/project/chelsa-cmip6/). This approach allows downscaling of global monthly climatologies of mean air temperature (tas), maximum air temperature (tasmax), minimum air temperature (tasmin), and precipitation (pr) and the calculation of nineteen bioclimatic variables plus growing degree days from the monthly climatologies. The CHELSA group (https://www.chelsa-climate.org/) has applied this method to downscale bias-corrected GCM output for a subset of CMIP6 models and scenarios. A brief description of this dataset can be

found at https://chelsa-climate.org/cmip6/ and the datasets themselves are available at https://envicloud.wsl.ch/#/?prefix=chelsa%2Fchelsa_V2%2FGLOBAL%2Fclimatologies%2F. For this work they started with ISIMIP3b datasets, which are GCM outputs to which the trend-preserving bias-correction of Lange (2019) has been applied, as described here: https://www.isimip.org/documents/413/ISIMIP3b_bias_adjustment_fact_sheet_Gnsz7CO.pdf. Thus the resulting CHELSA-downscaled datasets include bias-correction and downscaling. One drawback to this dataset, hereafter referred to as CHELSA_BC, is that it only contains global downscaled climatologies for four time periods (1981-2010, 2011-2040, 2041-2070, and 2071-2100), five GCMs (GFDL-ESM4, IPSL-CM6A-LR, MPI-ESM1-2-HR, MRI-ESM2-0, and UKESM1-0-LL), and three scenarios (SSP126, SSP370, SSP585). Another drawback is that the temperature datasets contain spatial interpolation artifacts stemming from the ISIMIP3b data which manifest as horizontal banding and gridding features and are especially apparent in polar regions.

The code for the CHELSA downscaling approach is publicly available (https://gitlabext.wsl.ch/karger/chelsa_cmip6/-/tree/master/), making it possible to downscale data for additional time periods, models, and scenarios. In this report we describe the modification of this code to downscale CMIP6 data for set time periods and for warming levels, for any model, ensemble member, or scenario. Note that the publicly available repository for the original CHELSA code only includes the downscaling used for CHELSA_BC, it does not include the bias correction. We also describe some evaluations of the resulting data, hereafter referred to as CHELSA_WW, relative to raw CMIP6 data, Daymet data (Thornton et al., 2022), and CHELSA_BC.

2. Downscaling Approach

2.1 CHELSA Downscaling Method

The CHELSA method is simple: it calculates temporal deltas in CMIP6 data and adds them to a high resolution reference dataset (Figure 1). Described in more detail, the CHELSA method imports CMIP6 data for a user specified model, ensemble member, and scenario for a reference period (1981-2010), an historical period (specified by the user), and a future period (specified by the user) and calculates monthly climatologies for each. Then deltas are calculated between the reference period and the historical period and between the reference period and the future period. The deltas are spatially interpolated to the grid of the 1 km resolution CHELSA reference data. The spatially interpolated CMIP6 deltas are finally added to the CHELSA reference data to create monthly climatologies at 1 km resolution for a historical and a future time period. Note that if the chosen historical period is the same as the reference period then the 1 km historical CMIP6 climatologies that the method produces will be the same as the CHELSA reference data. The provided code also automatically calculates nineteen bioclimatic variables plus growing degree days from the historical and future downscaled outputs.

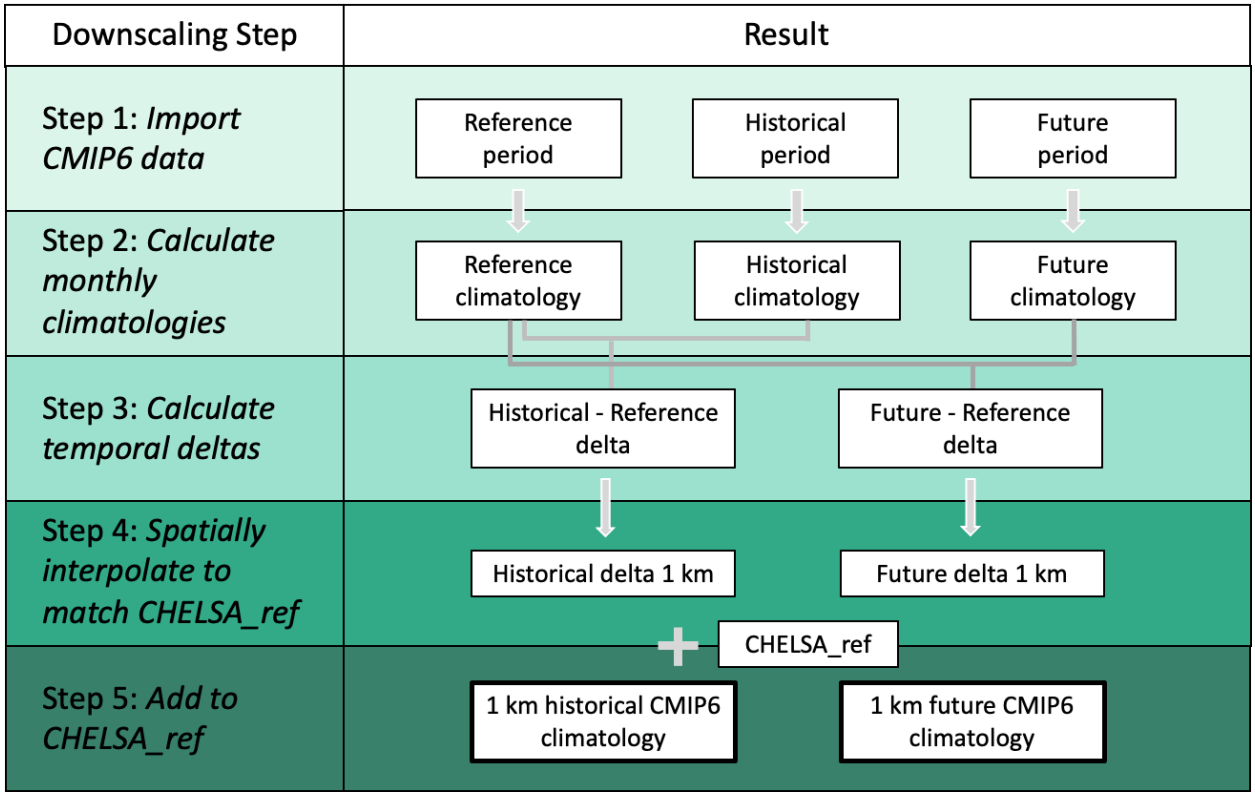

Figure 1. Diagram of the original CHELSA downscaling method. This process is replicated for each climate variable (tas, tasmax, tasmin, pr) and each model, ensemble member, and climate scenario. CHELSA_ref refers to the CHELSA reference data described in the text.

Version 1 of the CHELSA reference data includes monthly temperature and precipitation downscaled from ERA-Interim reanalysis data. Temperature was statistically downscaled from atmospheric temperature while precipitation was downscaled with consideration of orographic effects, valley exposition, and boundary layer height. A full description of the dataset and a comparison with other gridded and station data is available in Karger et al., (2017). Version 2 of the CHELSA reference data, which was used to create CHELSA_BC and CHELSA_WW, contains several modifications from Version 1. The biggest difference is that Version 2 is downscaled from ERA5 data. A full description of the CHELSA V2 reference data can be found in https://chelsa-climate.org/wp-admin/download-page/CHELSA_tech_specification_V2.pdf.

2.2 Modified CHELSA Downscaling Code

The CHELSA downscaling code is written in python and was downloaded from https://gitlabext.wsl.ch/karger/chelsa_cmip6/-/tree/master/. The code was modified as described below to better suit the needs of the Woodwell Risk Team.

Specifically, the code was modified to allow running in parallel using the dask map blocks approach, which maps across spatial tiles. Global runs are further chunked into three ‘hemispheres’ (north, middle, and south) to avoid memory issues.

The modified code can take a list of GCMs and downscale them in sequence. The code downloads CMIP6 data directly from Google Cloud. While the original code only ingested data available from the the standard collection (data listed in https://storage.googleapis.com/cmip6/cmip6-zarr-consolidated-stores.csv), the modified code allows the ingestion of files with low to medium errors as well (listed in https://storage.googleapis.com/cmip6/cmip6-zarr-consolidated-stores-noQC.csv). Low error levels are described as cases where the 'issue concerns file management (e.g., addition, removal, period extension, etc.)' while medium error levels are described as cases where the 'issue concerns metadata (netCDF attributes) without undermining the values of the involved variable'. Datasets with high or critical error levels are not ingested.

Unlike the original code, in which the user specifies an historical and a future time period to downscale, the modified code only downscales one time period at a time. This user-specified time period can be any past or future period available from the CMIP6 data, but we refer to it as the future period since that is the most common use case.The future period in the modified code can be specified as a date range or a warming level. If specified as a warming level, the warming level and model/member/scenario combination must be included in a csv file of warming years. The csv file must be formatted in the same way as the example csv file in the github repository, warming_years_zarr_21yr_window.csv. This example warming year csv file contains warming years for every model, member, and scenario combination in the Google Cloud store for warming levels 1°C, 1.5°C, 2°C, 2.5°C, 3°C, 3.5°C, 4°C, and 4.5°C. In this csv warming years were calculated as the midyear of the first 21 year period when time-averaged global mean surface temperature exceeded the warming level of interest relative to the pre-industrial period (1850-1900). The code is currently set up to ingest data for the 21 year period centered on this warming year. Modifications would need to be made to use warming years calculated using other approaches.

The modified code allows the user to specify whether they want to calculate the bioclimatic variables (nineteen bioclim variables plus growing degree days). Running the bioclimatic variables adds significant time to the overall computations; a run for a single model over a region covering 2° longitude and 10° latitude took 11 minutes, of which calculating the bioclimatic variables took 10 minutes (using one core on a virtual machine with 416GB memory). The bioclimatic variables also require considerable additional space; for the run described above, the combined size of the temperature and precipitation climatologies was 16 KB while the combined size of the bioclimatic variables was 24 MB.

Finally, the modified code automatically adds CF convention compliant metadata to the downscaled climatology datasets.

The modified CHELSA downscaling code is available at https://github.com/WoodwellRisk/CHELSA_downscaling.

3. CHELSA_WW Datasets

The modified CHELSA code was used to downscale CMIP6 data for three warming levels (1°C, 1.5°C, and 2°C) for two climate scenarios (SSP245 and SSP585). For these runs. 17 model/ensemble member combinations were considered for downscaling (Table 1). Data was available for all 17 models for SSP585, however for SSP245 data for ACCESS-ESM1-5 was unavailable. Warming years were calculated as the model specific 21 year window when time-averaged global mean surface temperature first exceeded the specified warming level. Bioclimatic variables were not calculated.

Model	Ensemble Member	SSP245	SSP585
ACCESS-CM2	r1i1p1f1		
ACCESS-ESM1-5	r1i1p1f1	n/a	
CanESM5	r1i1p1f1		
CNRM-CM6-1	r1i1p1f2		
CNRM-CM6-1-HR	r1i1p1f2		
CNRM-ESM2-1	r1i1p1f2		
EC-Earth3-Veg-LR	r1i1p1f1		
FGOALS-g3	r1i1p1f1		
GFDL-CM4	r1i1p1f1		
INM-CM4-8	r1i1p1f1		
INM-CM5-0	r1i1p1f1		
IPSL-CM6A-LR	r1i1p1f1		
MIROC6	r1i1p1f1		
MIROC-ES2L	r1i1p1f2		
MPI-ESM1-2-HR	r1i1p1f1		
MPI-ESM1-2-LR	r1i1p1f1		
MRI-ESM2-0	r1i1p1f1		

Table 1. Models and ensemble members downscaled at three warming levels (1°C, 1.5°C, and 2°C). n/a indicates the model/member was not available for the specified scenario and therefore was not downscaled.

These runs were completed on a Google Cloud VM configured as n1-highmem-64. The python environment used for the runs is outlined in the chelsa.yml file in the github repository.
Runs were split into three spatial domains as described above and run sequentially to avoid memory issues. Completing a global run for all models for a single scenario and warming level typically took around 30 hours. The code has also been used to downscale data for specific smaller domains (e.g. Ethiopia, Kampala, Kerala) and specific time periods (e.g. 1850-1900) as needed. The downscaled datasets are available upon request from the Woodwell RIsk Team.

4. Evaluation of CHELSA_WW

4.1 Comparison to CMIP6

We compared mean annual temperature and annual precipitation according to CHELSA_WW and CMIP6 for the CHELSA reference period (1981-2010) and a period reflecting a 2°C world. CMIP6 warming levels were calculated using the same approach as was used for CHELSA_WW, the first 21 year period when GMST exceeded the temperature threshold. For this comparison, we considered the multi-model mean of the 17 GCM/ensemble member combinations in Table 1 for only the SSP585 scenario.

4.1.1 Temperature

4.1.1.1 Reference Period (1981-2010)

Relative to the raw CMIP6 data, CHELSA_ref shows biases in annual temperature that exceed +/-3°C in places (Figure 2). The strongest positive biases are found in the Arctic and in the lower elevation areas adjacent to high elevation, complex terrain (e.g. the Tibetan Plateau). CHELSA_ref shows negative biases at the highest elevations and across much of the Southern Ocean. The pattern of positive and negative biases adjacent to and over complex terrain, respectively, can be explained by CHELSA_ref's finer spatial resolution (1 km) which better resolves the effects of elevation on air temperature.

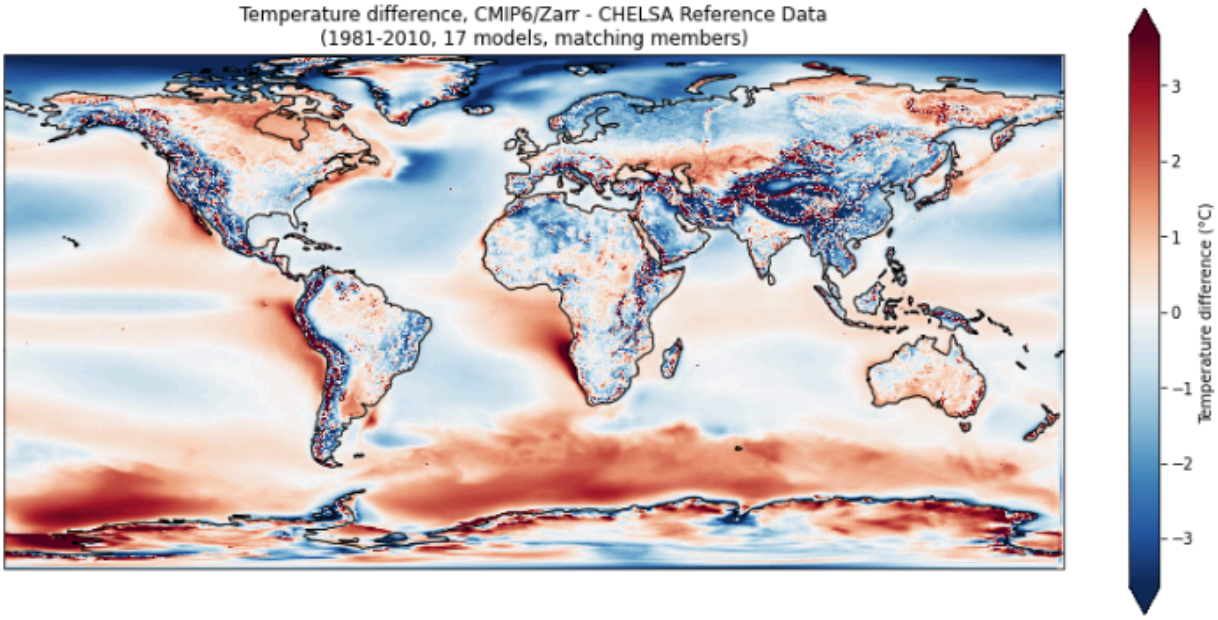

Figure 2. Difference in mean annual temperature between CHELSA_ref and CMIP6 for the 17 GCMs/ensemble members in Table 1 for the period 1981-2010.

Given that the CHELSA_ref data is downscaled from ERA5, we would expect CMIP6 biases relative to ERA5 to be similar to the biases shown above for CMIP6 relative to CHELSA_ref. Figure 3.3b of the IPCC AR6 Chapter 3 (https://www.ipcc.ch/report/ar6/wg1/figures/chapter-3/figure-3-3) shows the multi-model mean CMIP6 biases relative to ERA5 for the period 1995-2014 and is reproduced below (Figure 3). The CMIP6 biases relative to ERA5 are similar in spatial pattern and magnitude to the CMIP6 biases relative to CHELSA_ref (Figure 2).

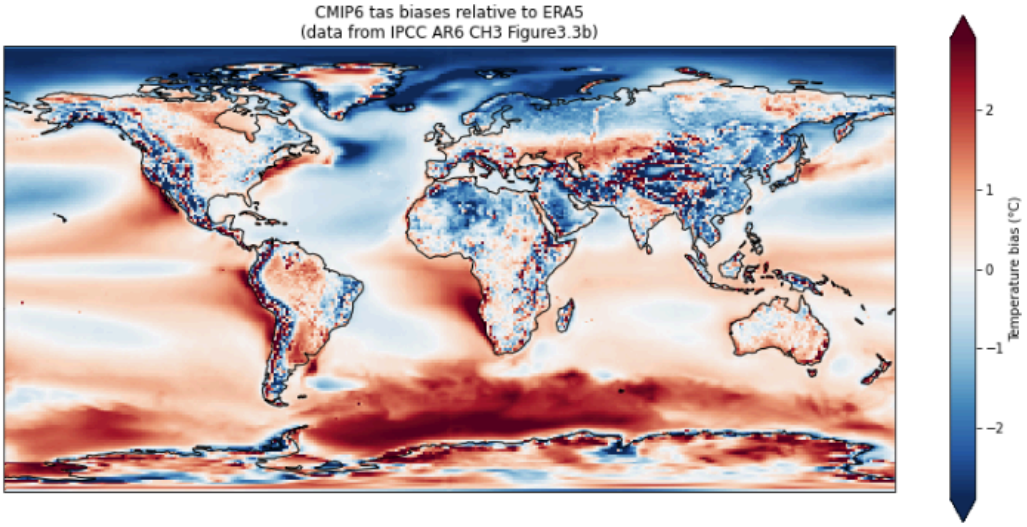

Figure 3. Biases in multi-model mean CMIP6 annual temperature relative to ERA5 for the period 1995-2014.

The difference between the two bias plots (Figure 4) is typically within +/-1°C and is partly attributable to differences in time periods and models used.

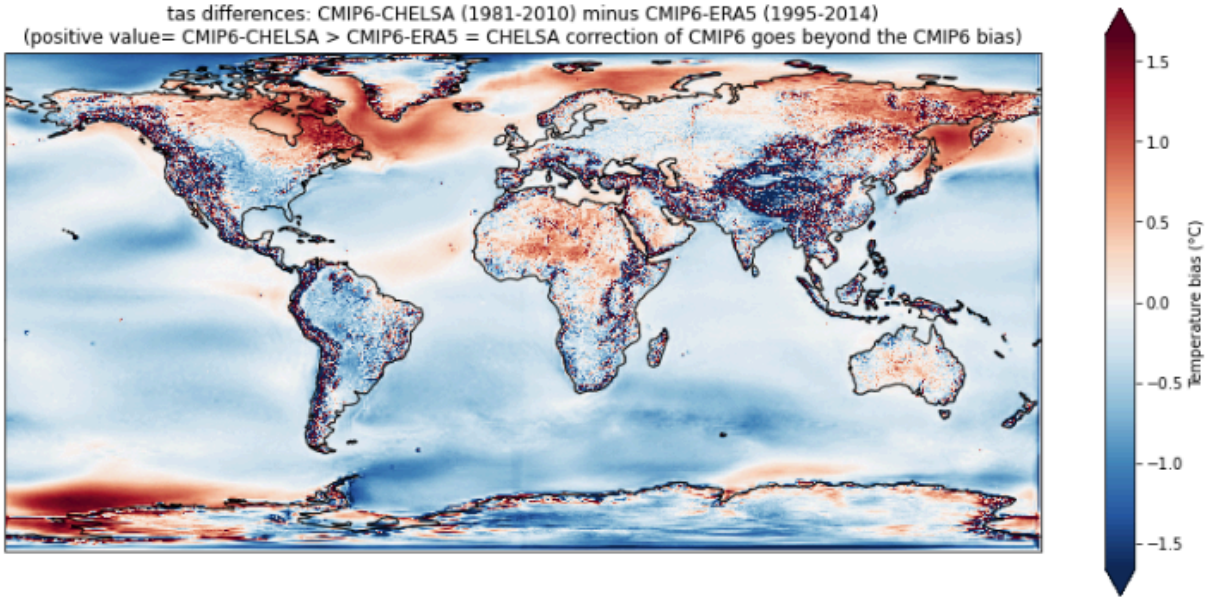

Figure 4. Comparison of previous two figures. This figure shows the CMIP6 bias relative to CHELSA (shown in Figure 2) minus the CMIP6 bias relative to ERA5 (shown in Figure 3). Note that this figure compares slightly different time periods and model ensembles.

4.1.1.2 SSP585 2°C Warming

Differences between CMIP6 and CHELSA in a 2°C world were the same as the differences between the two datasets in the reference period (Figure 5), which is expected based on the CHELSA downscaling algorithm.

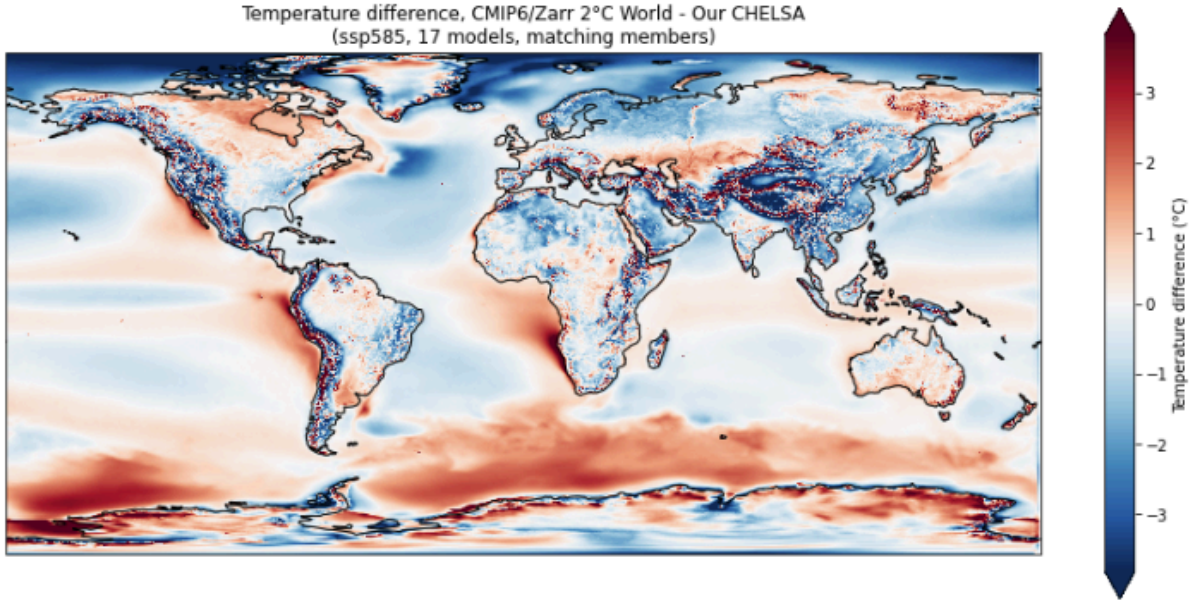

Figure 5. Difference in mean annual temperature between CMIP6 and CHELSA_WW in a 2°C world.

4.1.2 Precipitation

4.1.2.1 Reference Period (1981-2010)

For annual precipitation, CHELSA_ref differences from CMIP6 are of mixed signs (Figures 6 and 7). The largest absolute positive biases in CHELSA_ref (opposite of image below) are found over equatorial ocean regions and the south Atlantic. The largest relative negative biases in CHELSA_ref are concentrated in offshore coastal areas and dry areas such as the Sahara Desert. CMIP6 appears to be biased dry on windward slopes of major mountain ranges and biased wet on leeward slopes relative to CHELSA_ref, suggesting that CHELSA_ref's finer resolution is resolving some orographic effects that CMIP6 models cannot.

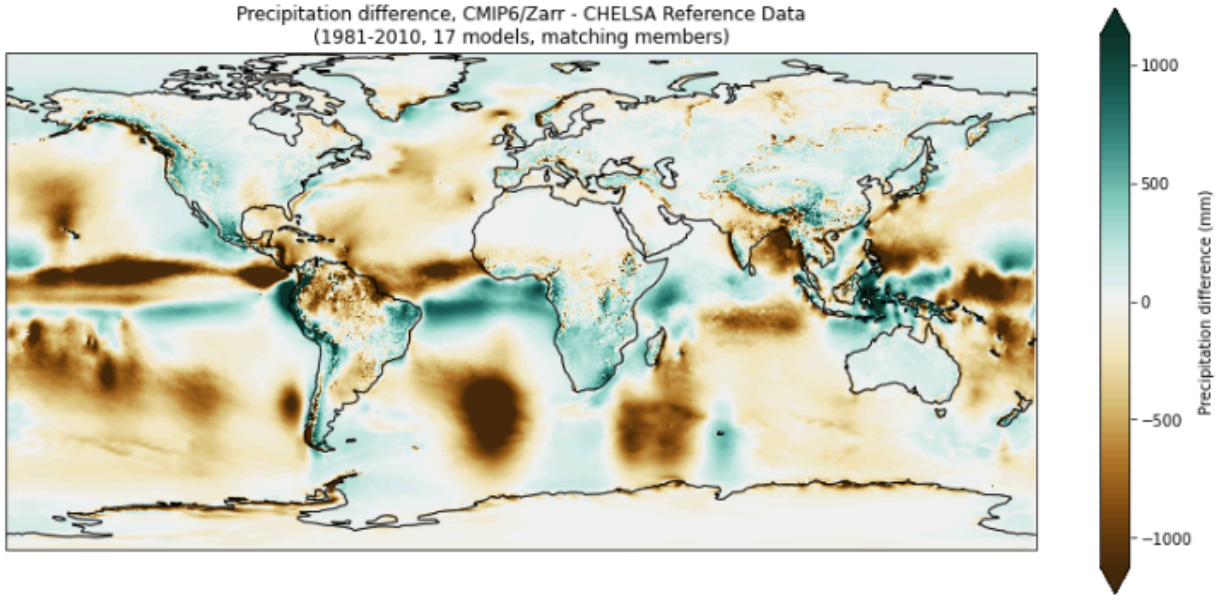

Figure 6. Difference in mean annual precipitation between CMIP6 and CHELSA_ref during the period 1981-2010.

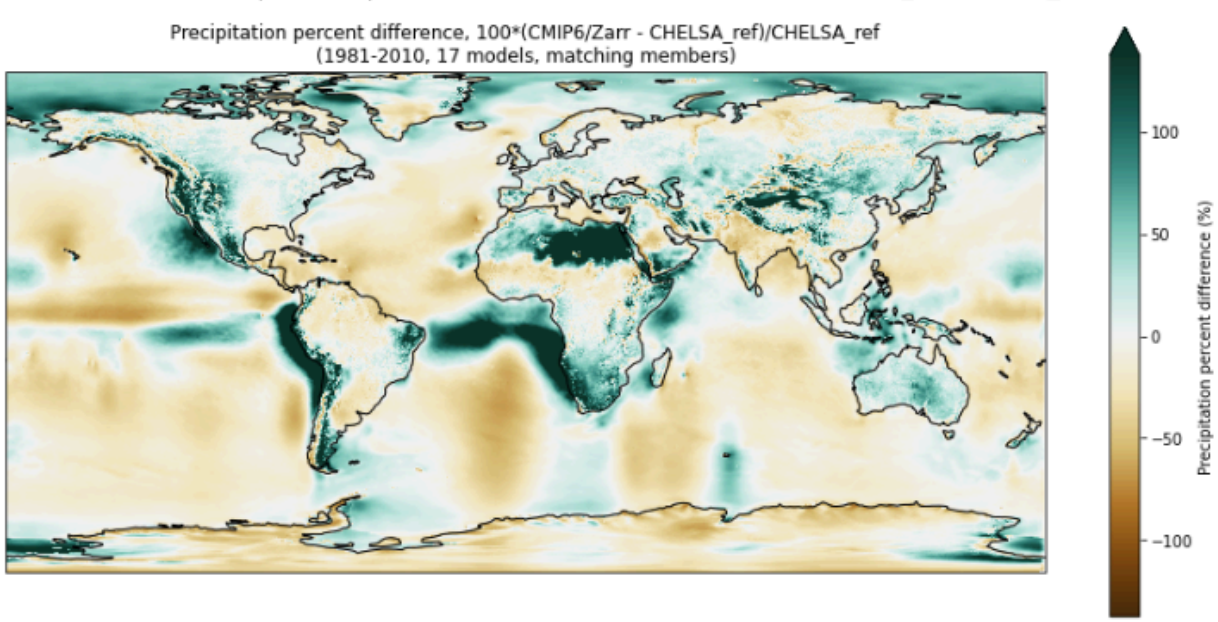

Figure 7. Percent difference in mean annual precipitation between CMIP6 and CHELSA_ref during the period 1981-2010.

4.1.2.2 SSP585 2°C Warming

The differences between CMIP6 and CHELSA_WW in a 2°C world were the same as those in the reference period (Figures 8 and 9), as expected based on the CHELSA downscaling algorithm.

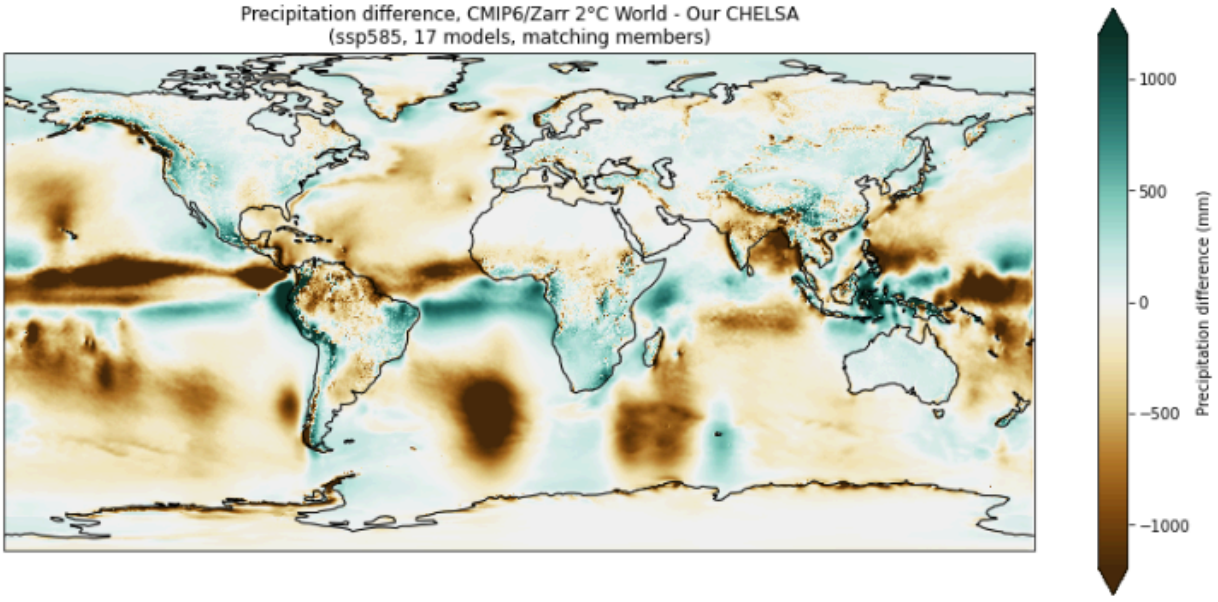

Figure 8. Difference in mean annual precipitation between CMIP6 and CHELSA_WW in a 2°C world.

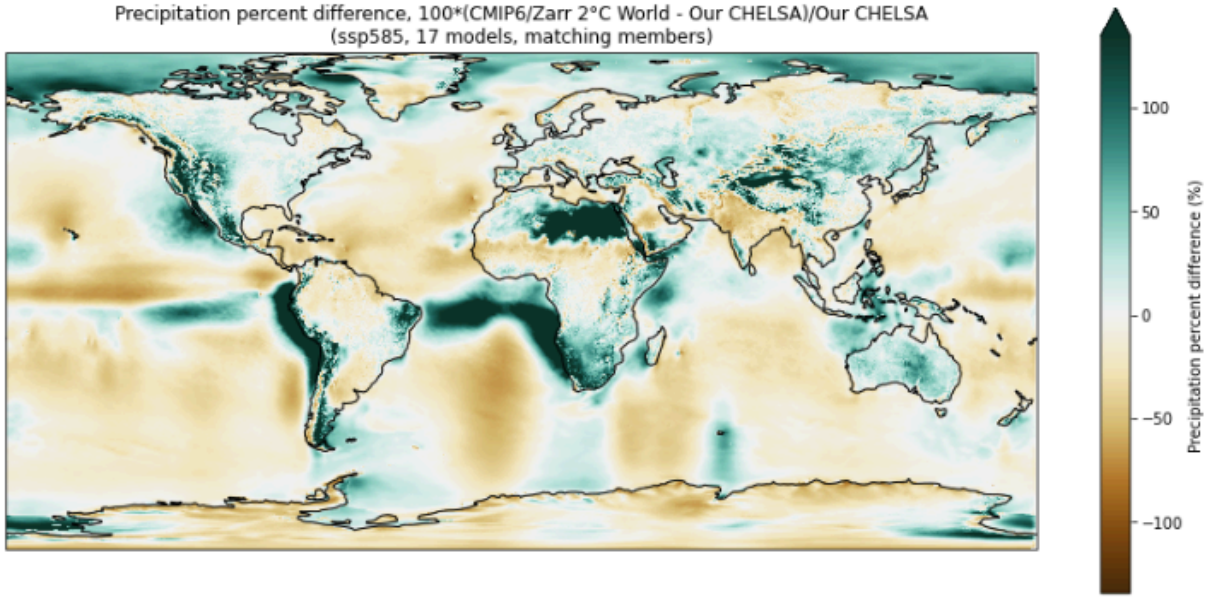

Figure 9. Percent difference in mean annual precipitation between CMIP6 and CHELSA_WW in a 2°C world.

4.2 Comparison to Daymet

We compared mean annual temperature and annual precipitation from the CHELSA_WW dataset to the Daymet V4 dataset (https://daymet.ornl.gov/). Daymet interpolates and extrapolates ground observations to provide 1 km resolution gridded historical climate data for North America, Hawaii, and Puerto Rico. Comparisons were completed for two regions: the Northeast US, to capture coastal effects, and an area centered on Idaho, to evaluate CHELSA_WW performance in complex terrain. Comparisons were completed for two time periods. We first compared data for the CHELSA reference time period (1981-2010). For this time period CHELSA_WW is the same as CHELSA_ref, providing a useful preliminary comparison. We then compared data for a 1°C world. This comparison looked at CHELSA data downscaled from CMIP6 for model-specific 21-year windows as described above for SSP585 and compared that data to Daymet data for the period 2000-2020, which roughly corresponds to 1°C warming since pre-industrial times. In the figures in this section, ‘CHELSA-CMIP6’ refers to CHELSA_WW.

4.2.1 Temperature

4.2.1.1 Reference Period (1981-2010)

During the reference period, mean temperature from CHELSA_WW is warmer (on the order of 0-1°C warmer) than Daymet in most parts of the Northeast US in all months and at the annual scale (Figures 10 and 11). Large warm and cool biases, depending on the month, are visible over Lake Ontario. Only small areas of cool biases over land are visible. Biases do not appear

to be related to coastal influence as the magnitude of biases is similar near the coast and further inland.

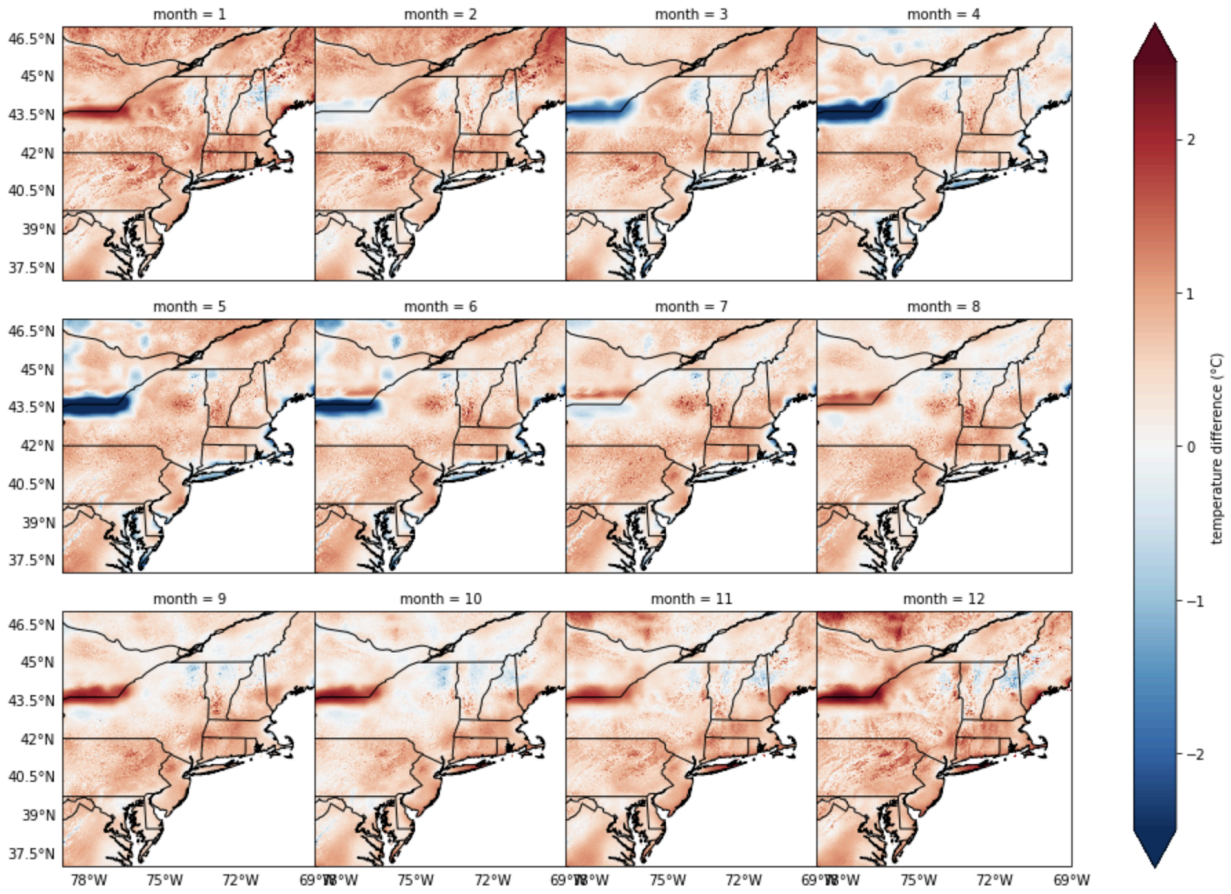

Figure 10. Difference in monthly average temperature, CHELSA_WW minus Daymet, for the Northeast US for the period 1981-2010.

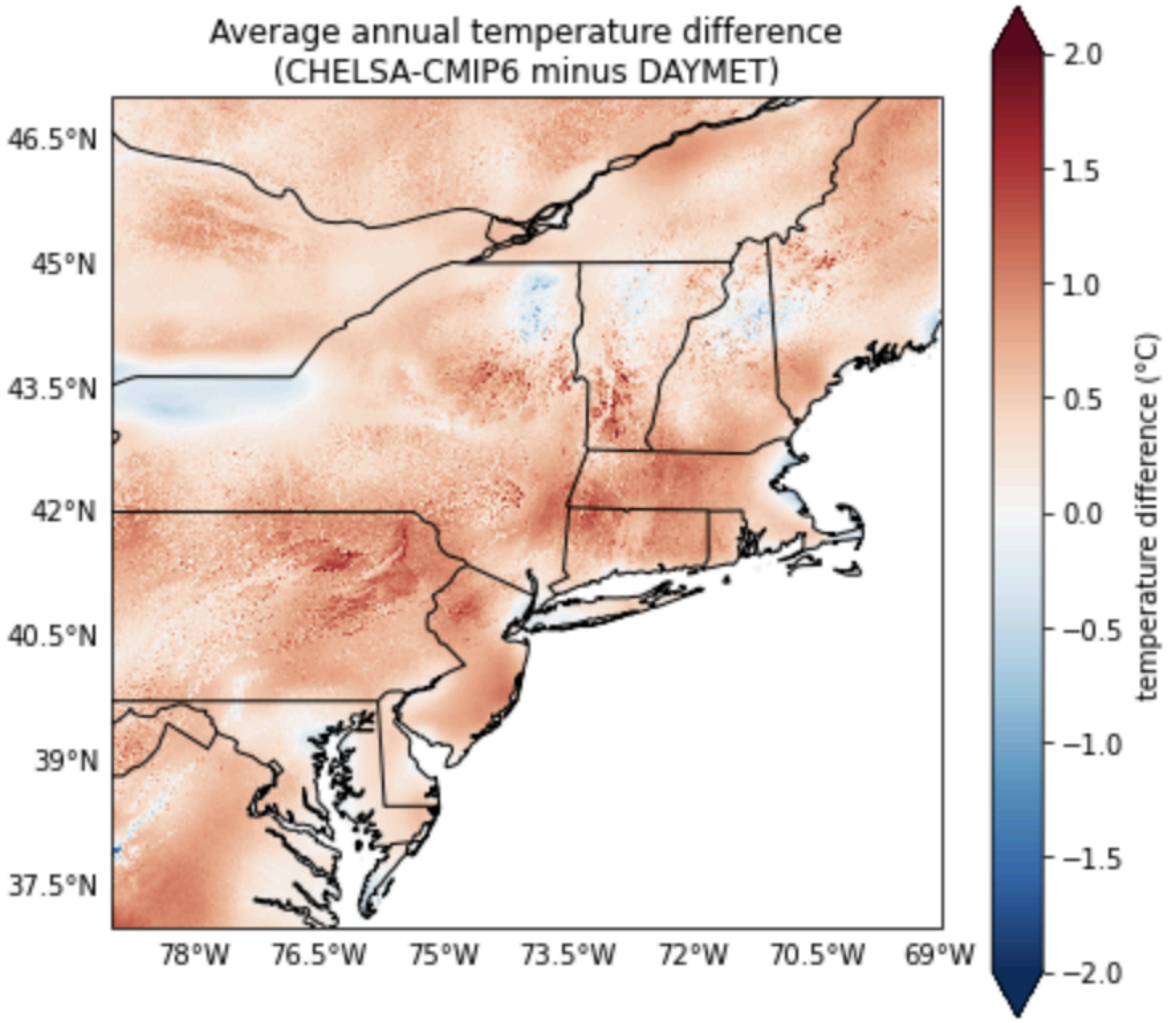

Figure 11. Difference in annual average temperature, CHELSA_WW minus Daymet, for the Northeast US for the period 1981-2010.

Over Idaho, reference period differences between CHELSA_WW and Daymet mean temperature display clear elevational and seasonal patterns (Figures 12 and 13). At high elevations, CHELSA_WW is as much as 4°C cooler than Daymet in the winter, with weaker contrasts in the summer months. At low elevations, CHELSA_WW is as much as 4°C warmer than Daymet in the summer, with weaker contrasts in the winter. At the annual scale this results in cool biases at high elevations and warm biases at low elevations relative to Daymet. The correlation between annual temperature bias and elevation is -0.68. This strong relationship may indicate differences in the treatment of temperature lapse rates in the two datasets.

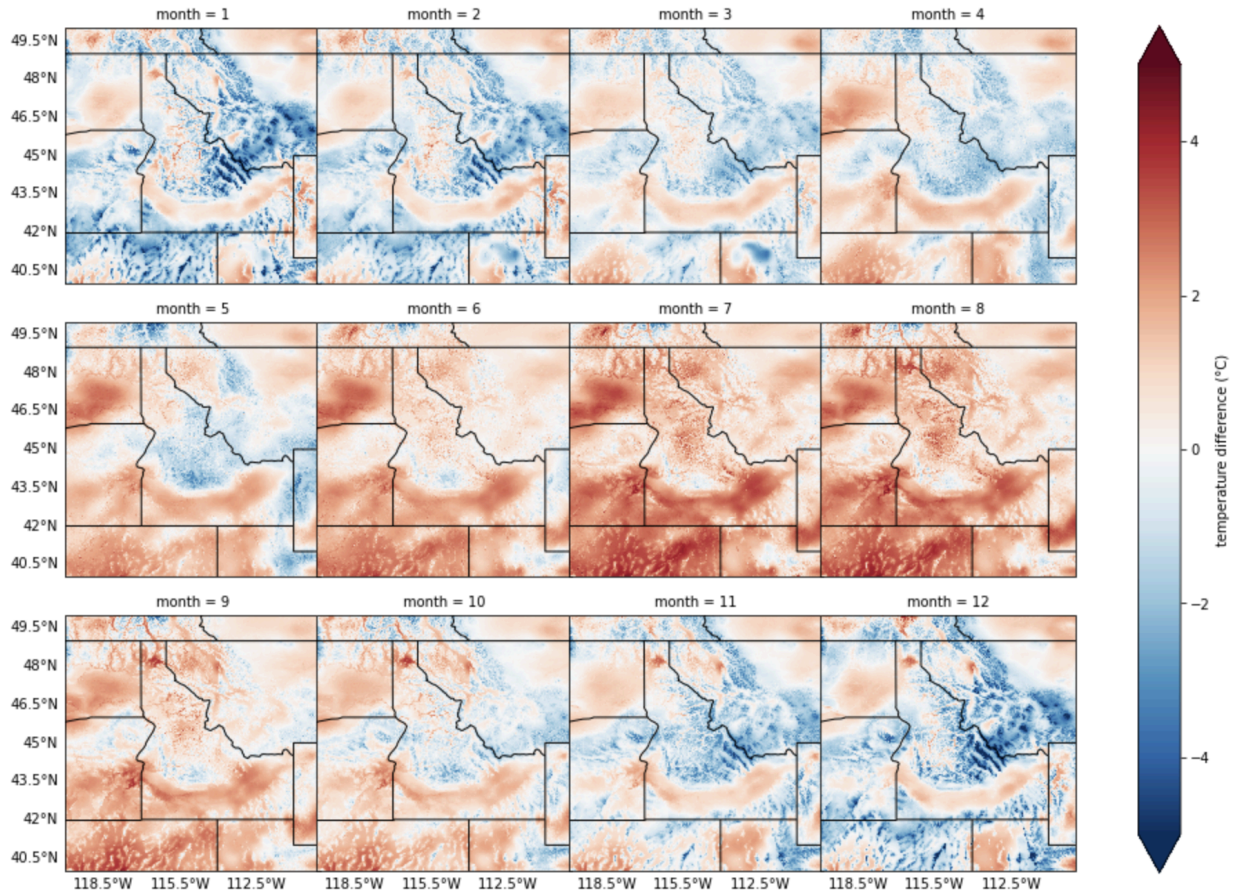

Figure 12. Difference in monthly average temperature, CHELSA_WW minus Daymet, for a region centered on Idaho for the period 1981-2010.

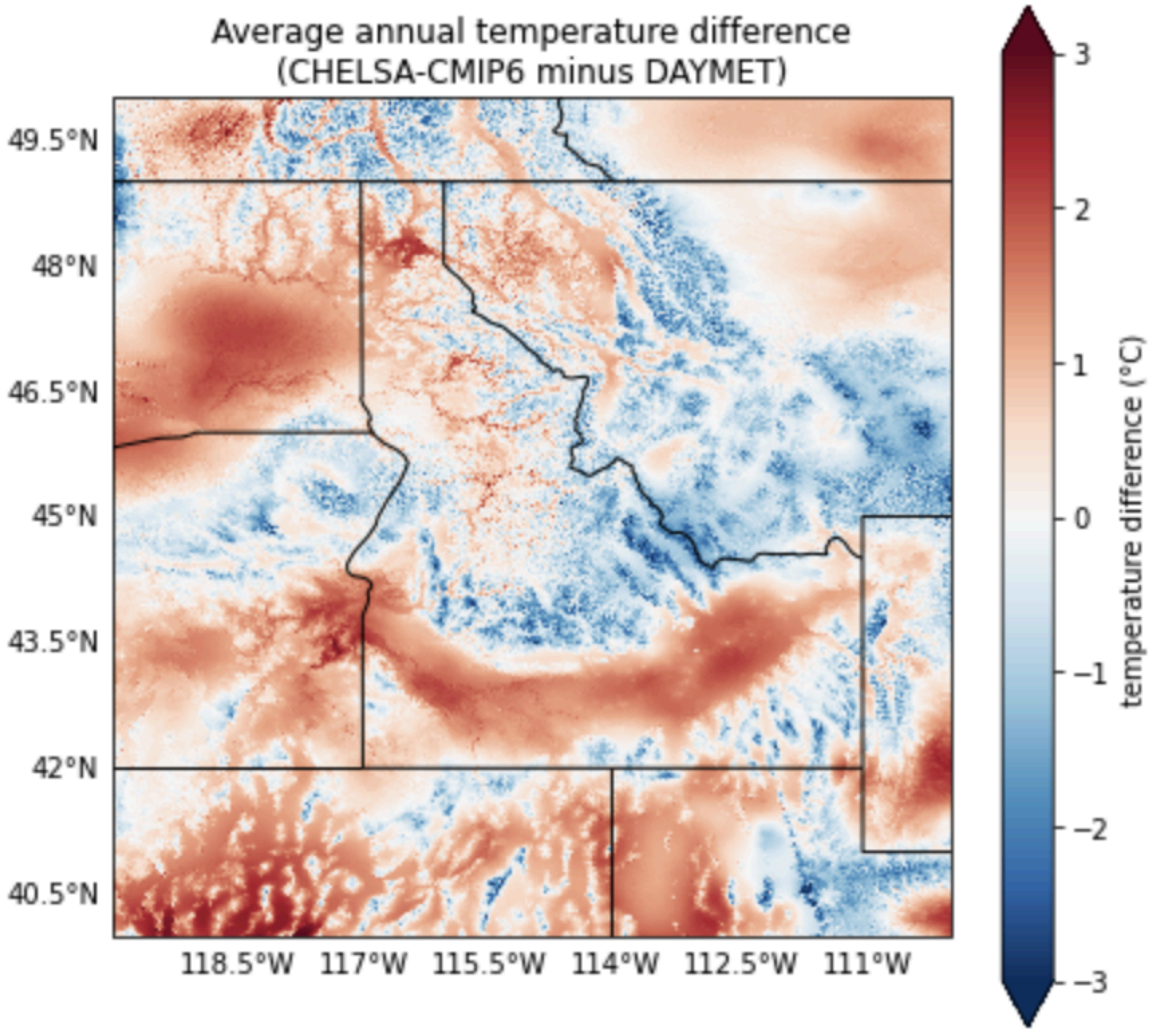

Figure 13. Difference in annual average temperature, CHELSA_WW minus Daymet, for a region centered on Idaho for the period 1981-2010.

4.2.1.2 SSP585 1°C Warming

For the Northeast US, monthly temperature biases in a 1°C world (Figures 14 and 15) are similar to, but stronger than, those in the reference period. Warm biases are particularly strong in February, when they exceed 2°C in some locations. Annual biases are almost universally positive.

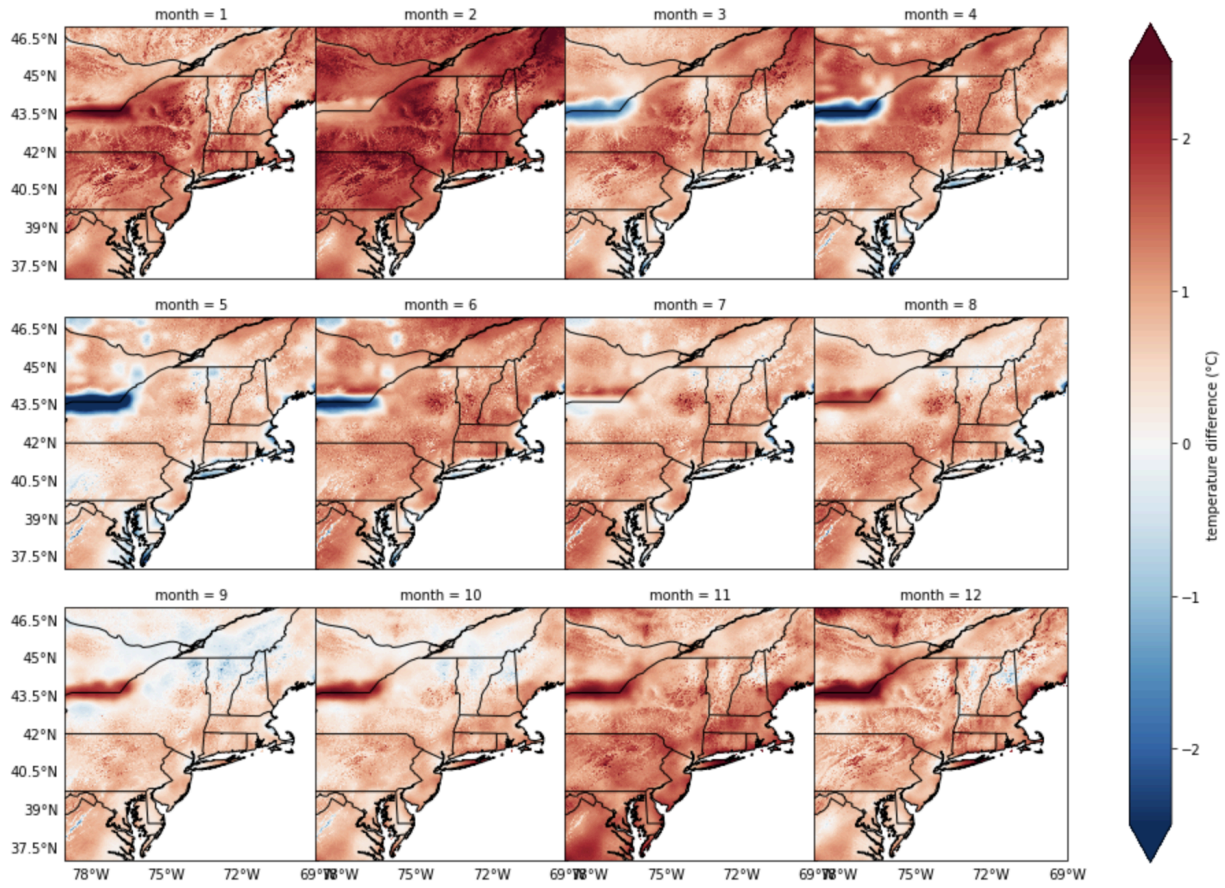

Figure 14. Difference in monthly average temperature, CHELSA_WW minus Daymet, for the Northeast US for the period reflecting 1°C warming.

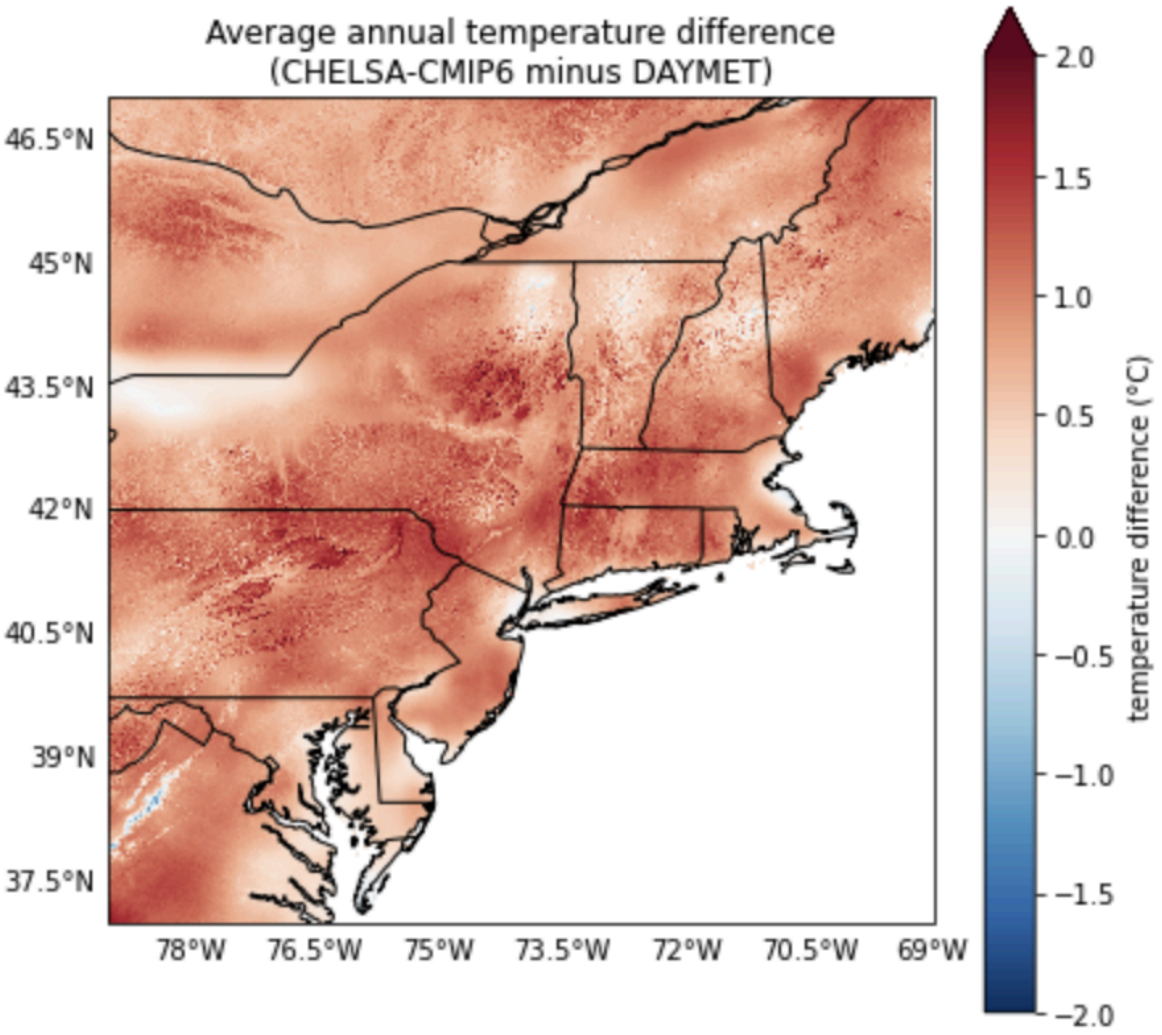

Figure 15. Difference in annual average temperature, CHELSA_WW minus Daymet, for the Northeast US for the period reflecting 1°C warming.

For the region centered on Idaho, biases relative to Daymet in a 1°C world (Figures 16 and 17) are similar in elevational and seasonal pattern to those in the reference period. Biases in a 1°C world are slightly stronger, which is most visible at the annual scale.

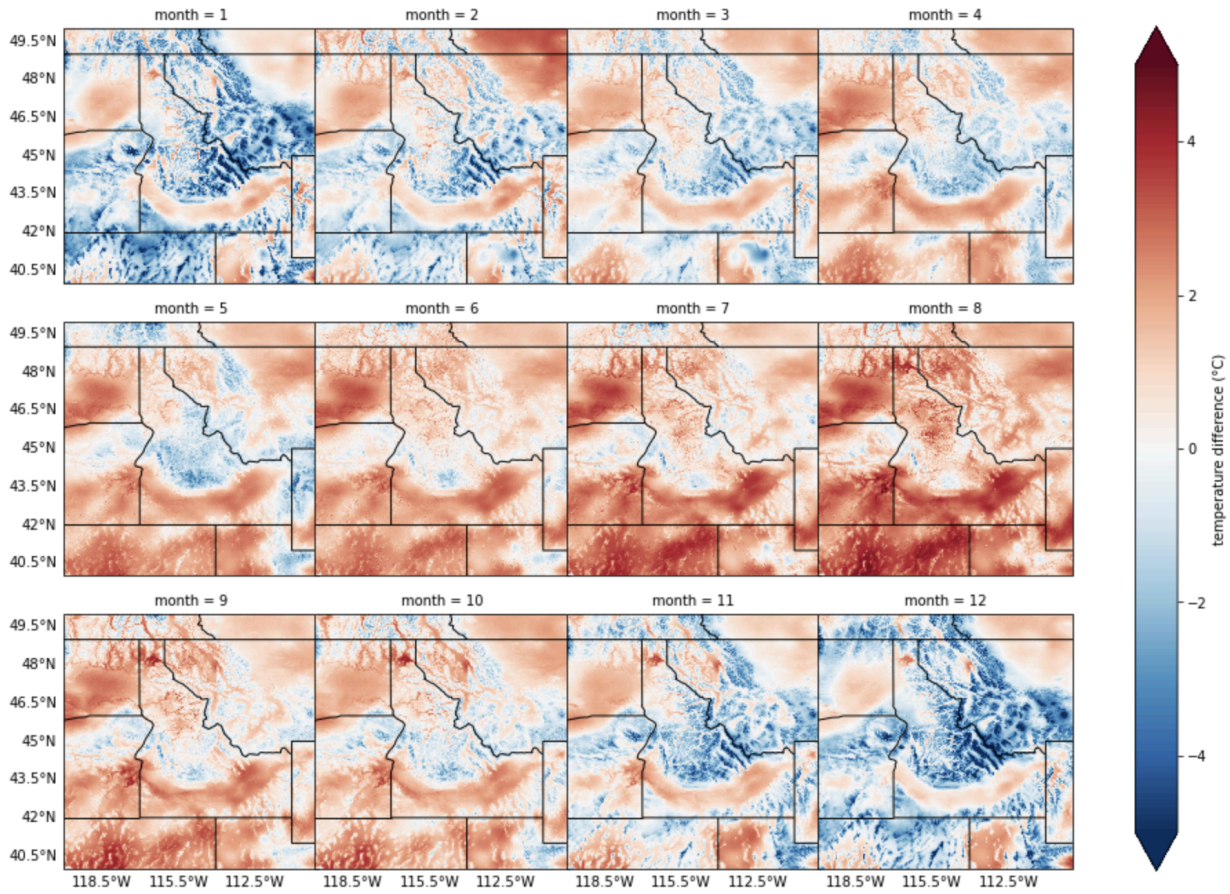

Figure 16. Difference in monthly average temperature, CHELSA_WW minus Daymet, for a region centered on Idaho for the period reflecting 1°C warming.

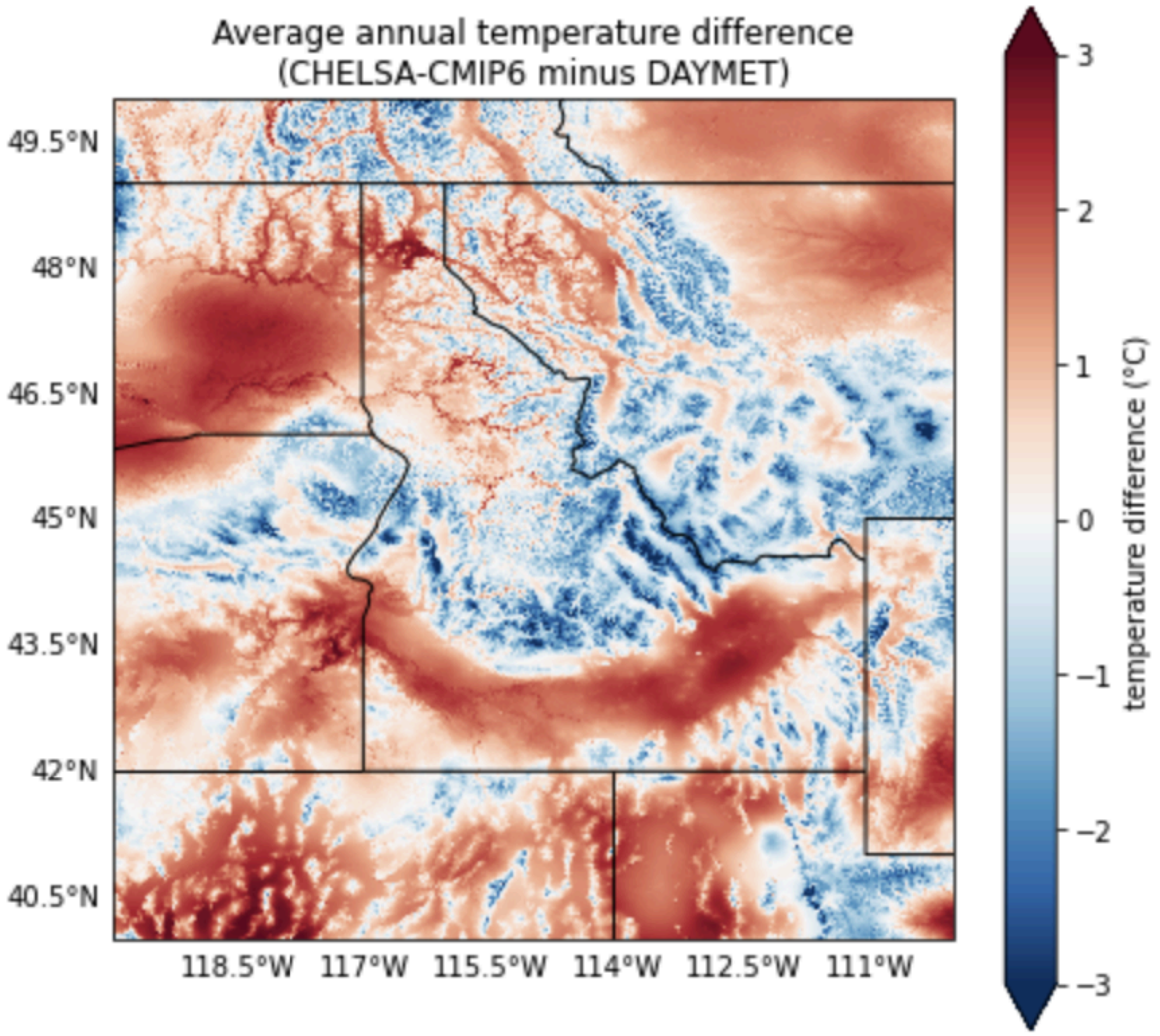

Figure 17. Difference in annual average temperature, CHELSA_WW minus Daymet, for a region centered on Idaho for the period reflecting 1°C warming.

4.2.2 Precipitation

4.2.2.1 Reference Period (1981-2010)

Patterns of percent difference in monthly precipitation during the reference period between CHELSA_WW and Daymet are spatially and temporally mixed in the Northeast US (Figures 18 and 19). One consistent feature is a dry bias in the northwest corner of the domain. Annual precipitation biases are spatially mixed and typically less than +/- 20%.

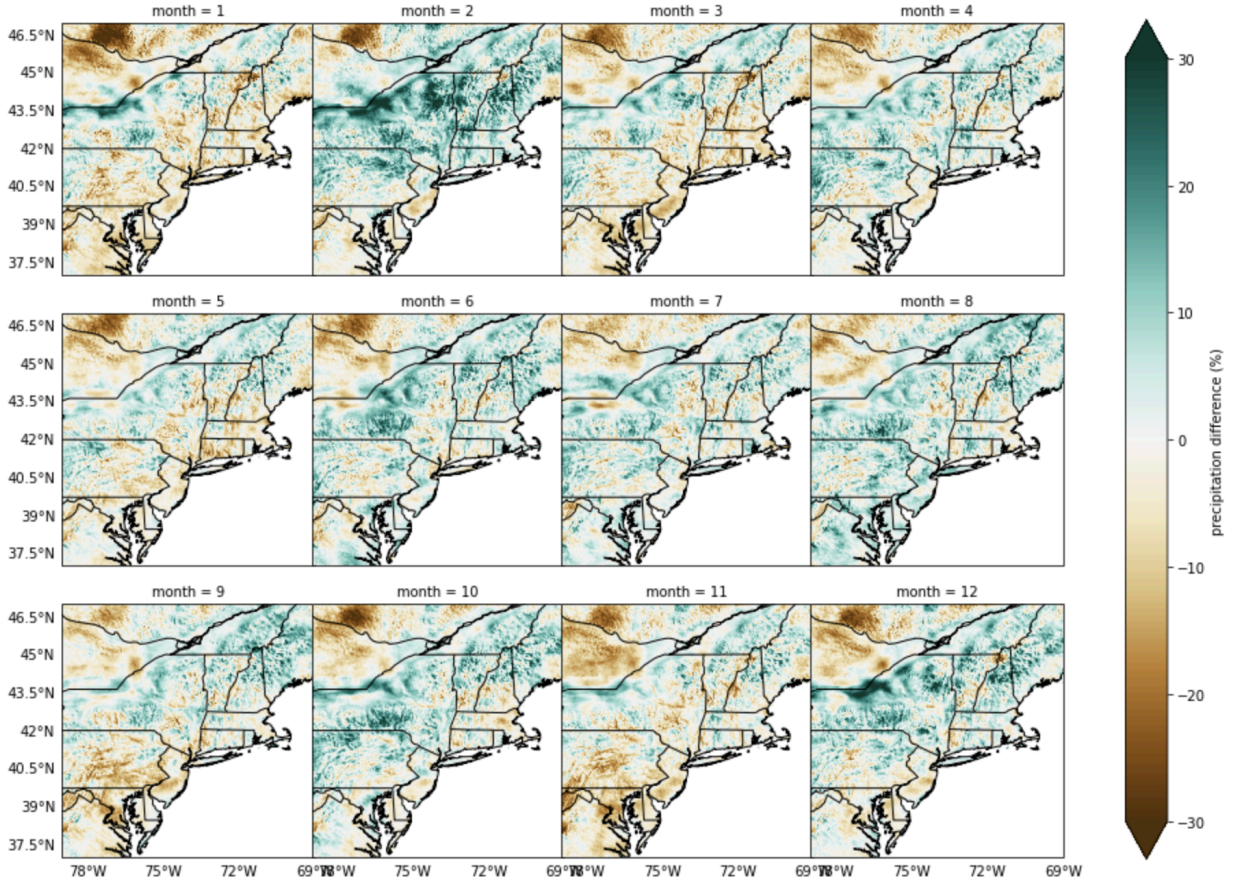

Figure 18. Difference in monthly precipitation, CHELSA_WW minus Daymet divided by Daymet, for the Northeast US for the period 1981-2010.

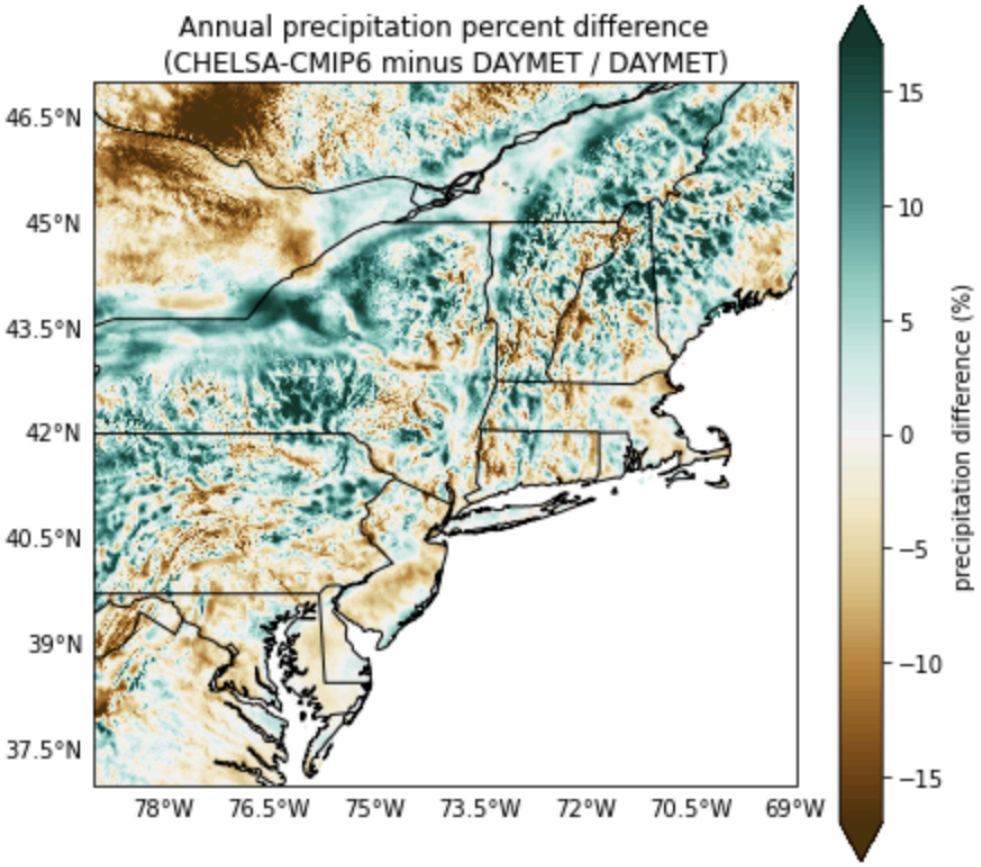

Figure 19. Difference in annual precipitation, CHELSA_WW minus Daymet divided by Daymet, for the Northeast US for the period 1981-2010.

For the region centered on Idaho, reference period precipitation biases relative to Daymet are somewhat spatially mixed, but are predominantly negative in the winter months (November-March) and predominantly positive in the summer months (June-September) (Figures 20, 21). The strongest biases are found at high elevations. Annual biases are of mixed sign, but typically less than +/- 40%.

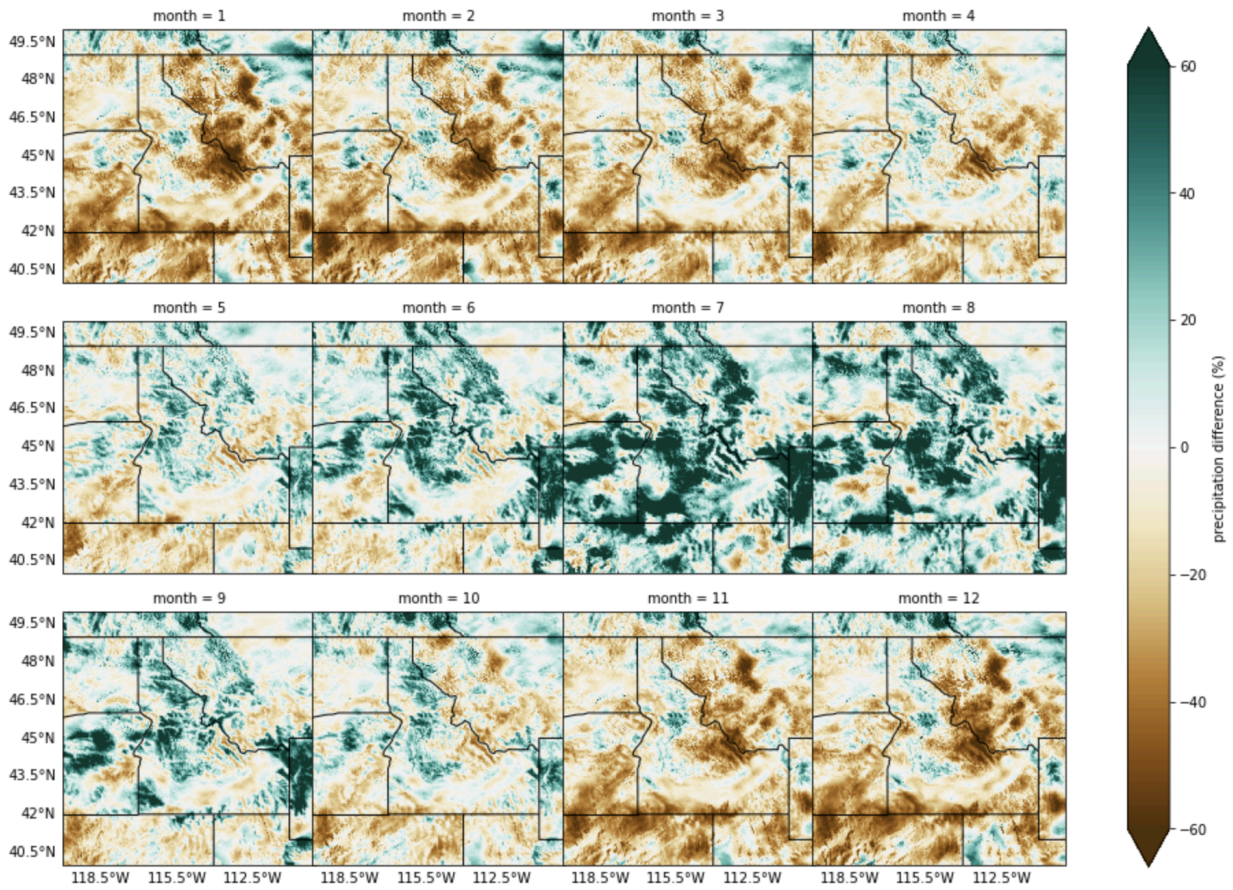

Figure 20. Difference in monthly precipitation, CHELSA_WW minus Daymet divided by Daymet, for a region centered on Idaho for the period 1981-2010.

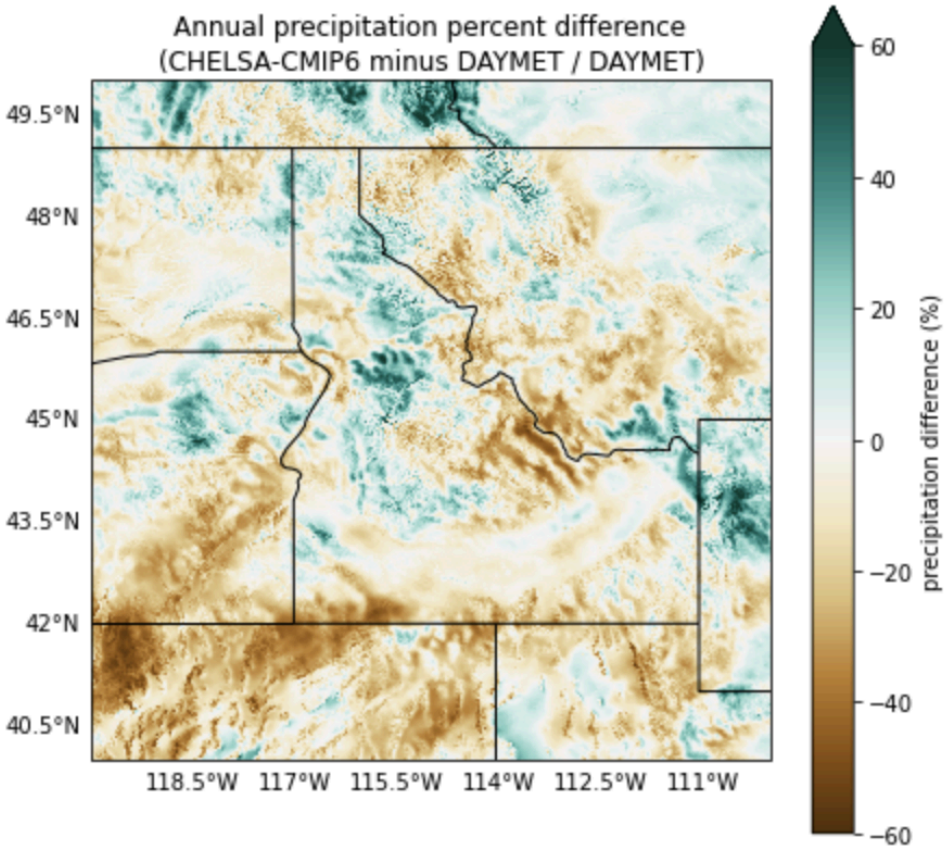

Figure 21. Difference in annual precipitation, CHELSA_WW minus Daymet divided by Daymet, for a region centered on Idaho for the period 1981-2010.

4.2.2.2 SSP585 1°C Warming

Northeast US precipitation biases are generally stronger in a 1°C world than in the reference period (Figures 22 and 23). Positive biases are most apparent in January and November, whereas negative biases are most widespread in October. The stronger monthly biases cancel out to some extent, making annual biases similar in a 1°C world to those in the reference period.

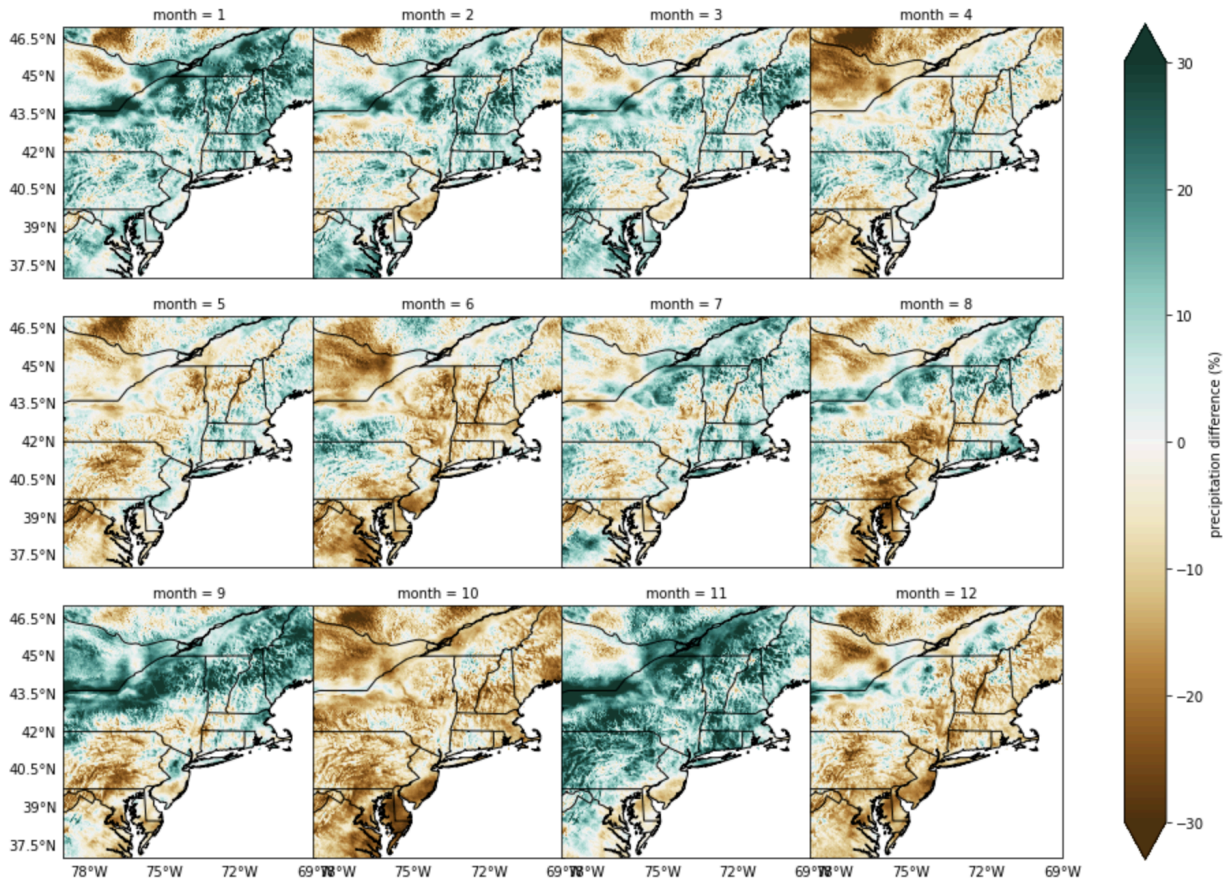

Figure 22. Percent difference in monthly precipitation, CHELSA_WW minus Daymet divided by Daymet, for the Northeast US for the period reflecting 1°C warming.

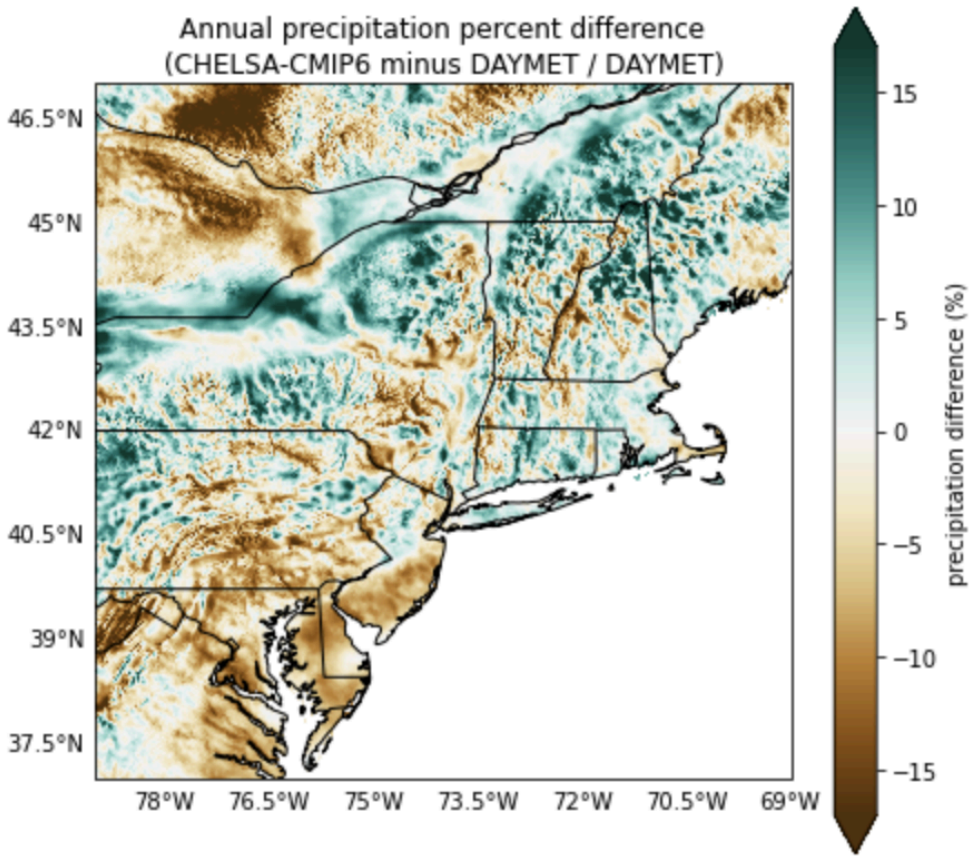

Figure 23. Percent difference in annual precipitation, CHELSA_WW minus Daymet divided by Daymet, for the Northeast US for the period reflecting 1°C warming.

For the Idaho region, precipitation biases relative to Daymet are more negative in the winter and shoulder seasons, switching to positive in the dry summer months (Figures 24 and 25). The magnitude and spatial pattern of annual precipitation biases is similar to the reference period.

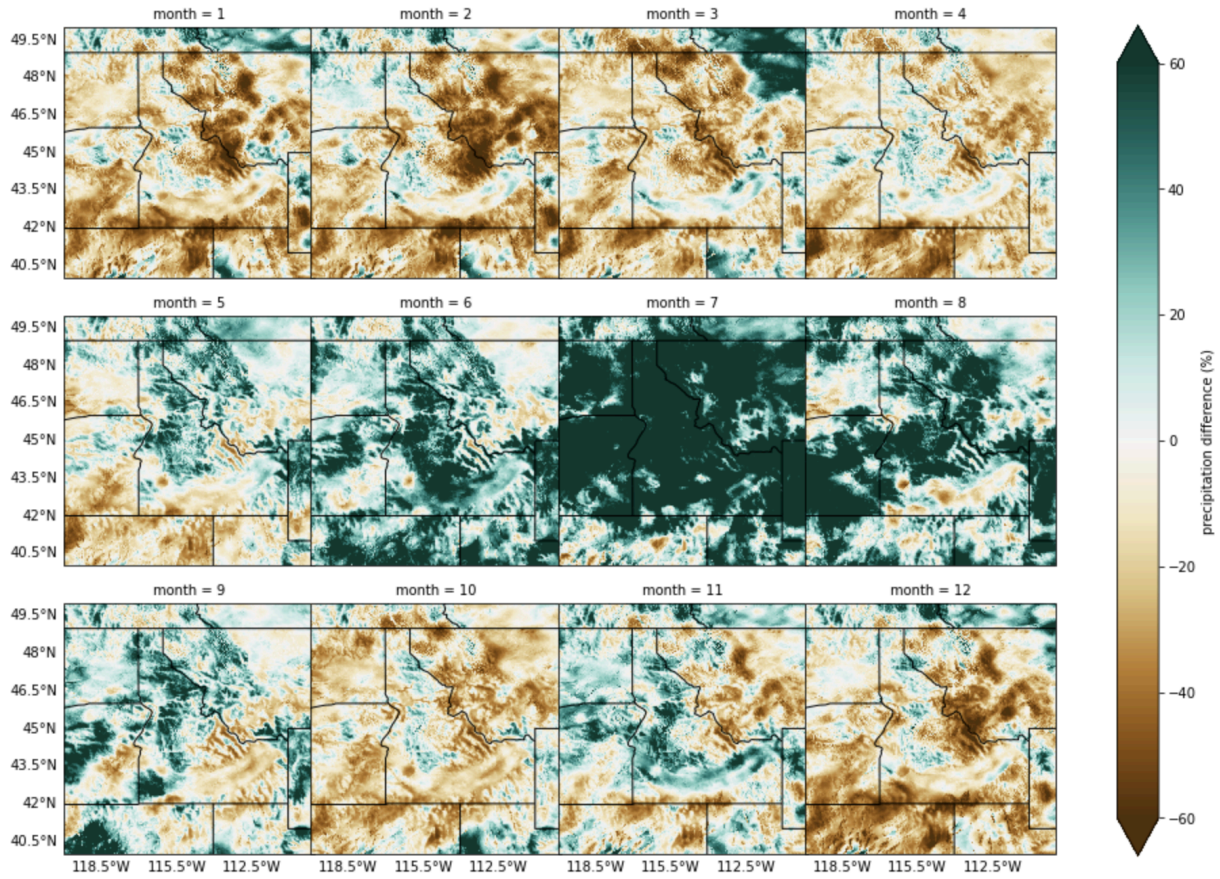

Figure 24. Percent difference in monthly precipitation, CHELSA_WW minus Daymet divided by Daymet, for a region centered on Idaho for the period reflecting 1°C warming.

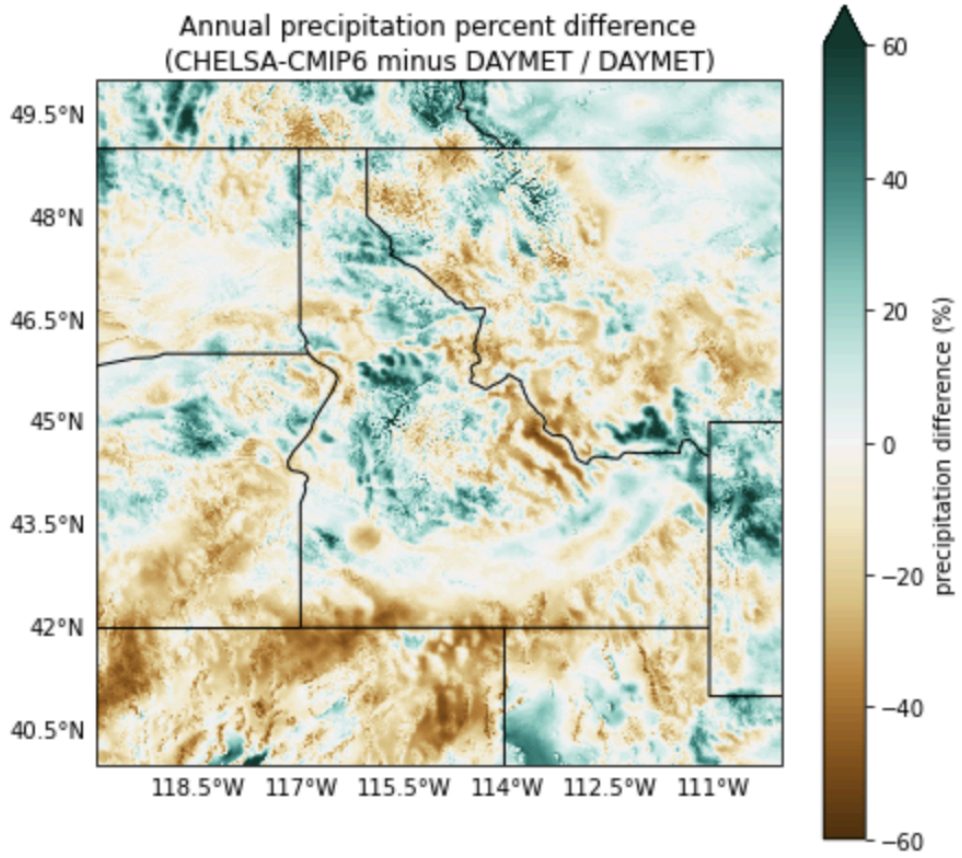

Figure 25. Percent difference in annual precipitation, CHELSA_WW minus Daymet divided by Daymet, for a region centered on Idaho for the period reflecting 1°C warming.

4.3 Comparison to CHELSA_BC

In a final set of evaluations of the CHELSA_WW product, CHELSA_WW was compared to the published CHELSA product, CHELSA_BC, available here: https://envicloud.wsl.ch/#/?prefix=chelsa%2Fchelsa_V2%2FGLOBAL%2Fclimatologies%2F. Differences between CHELSA_WW and CHELSA_BC stem from the use of raw CMIP6 data in CHELSA_WW vs the use of bias-corrected CMIP6 data from ISIMIP3b in CHELSA_BC. The comparisons considered the multi-model mean of the three GCMs available from CHELSA_BC that are also in Table 1 (IPSL-CM6A-LR, MRI-ESM2-0, and MPI-ESM1-2-HR) for SSP585 for two time periods (2041-2070 and 2071-2100).

4.3.1 Temperature

4.3.1.1 SSP585 2041-2070

For the midcentury period (2041-2070), mean annual temperature differences between CHELSA_BC and CHELSA_WW were typically less than +/- 0.2°C, especially over land areas (Figure 26). Over most land areas CHELSA_BC was slightly cooler than CHELSA_WW.

Horizontal banding in the difference plot below stems from the CHELSA_BC data and is a known artifact of the ISIMIP3b data.

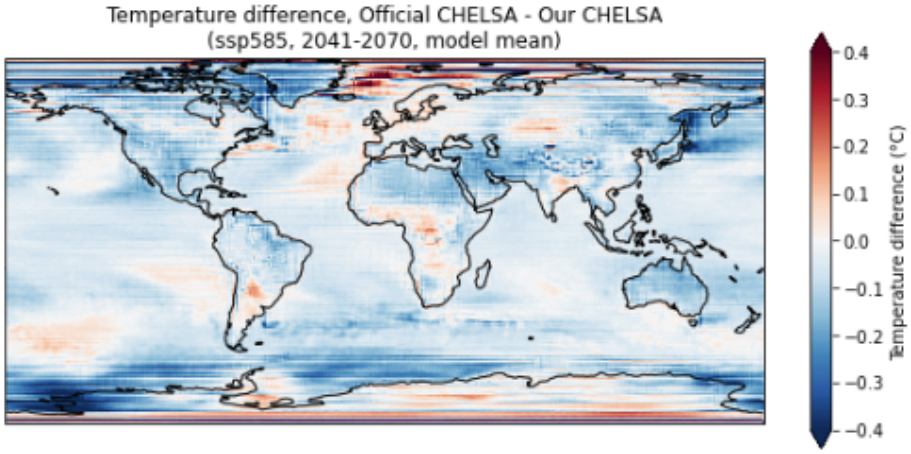

Figure 26. Difference in mean annual temperature between CHELSA_BC and CHELSA_WW for 2041-2070, averaged across three models.

Temperature differences between the two datasets were model dependent. Out of the three models, the largest contrasts were seen for MPI-ESM1-2-HR (Figure 27) while the other two models had similarly small temperature differences.

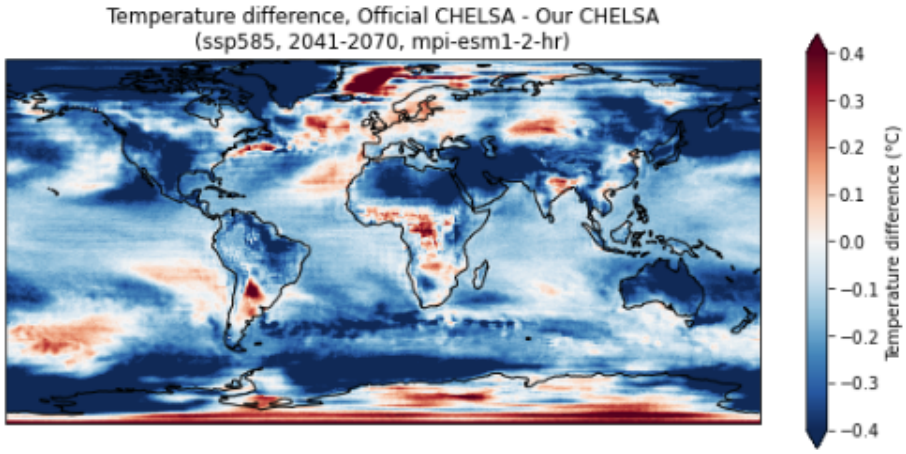

Figure 27. Difference in mean annual temperature between CHELSA_BC and CHELSA_WW for 2041-2070 for the MPI-ESM1-2-HR model.

4.3.1.2 2071-2100

Differences in mean annual temperature between CHELSA_BC and CHELSA_WW for the late 21st century period (Figure 28) were similar to those for the midcentury period. The MPI-ESM1-2-HR model again showed the largest temperature differences of the three models.

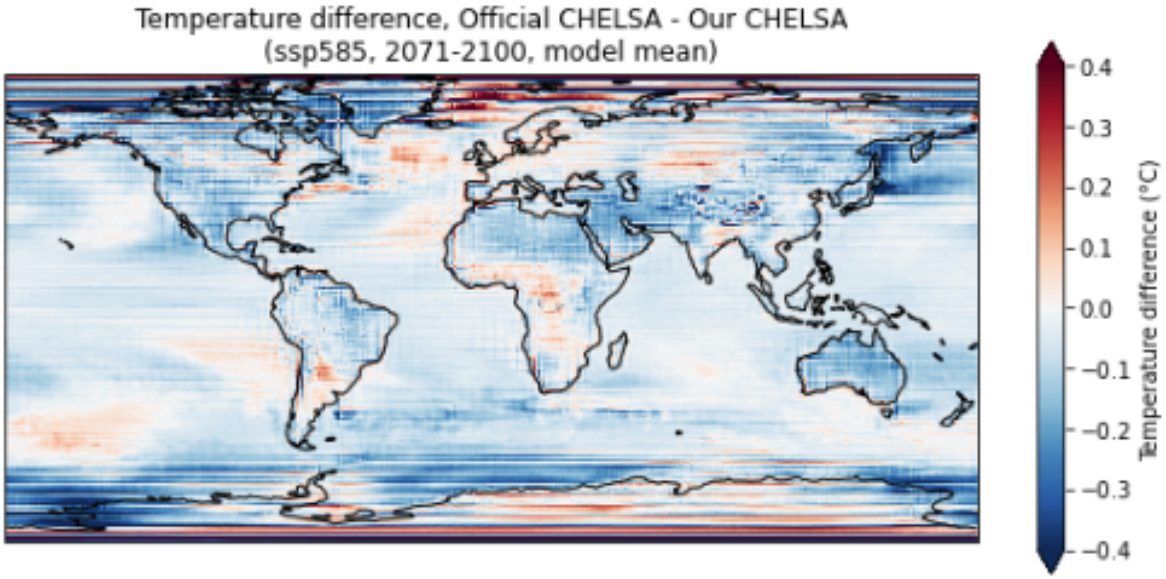

Figure 28. Difference in mean annual temperature between CHELSA_BC and CHELSA_WW for 2071-2100, averaged across three models.

4.3.2 Precipitation

4.3.2.1 2041-2070

Absolute differences in precipitation between CHELSA_BC and CHELSA_WW for the period 2041-2070 are largest over equatorial ocean regions (> +/- 15 mm in places) (Figure 29). Over land areas, differences are typically within +/- 5 mm. Percent differences in annual precipitation are largest over equatorial ocean regions where differences of mixed signs are seen (> +/-20%), and over polar regions and the Sahara Desert, where CHELSA_BC is drier than CHELSA_WW by more than 20% in cases (Figure 30). Unlike temperature, there was not a single model that contributed most of the differences; all models had similar magnitudes of contrast between CHELSA_BC and CHELSA_WW.

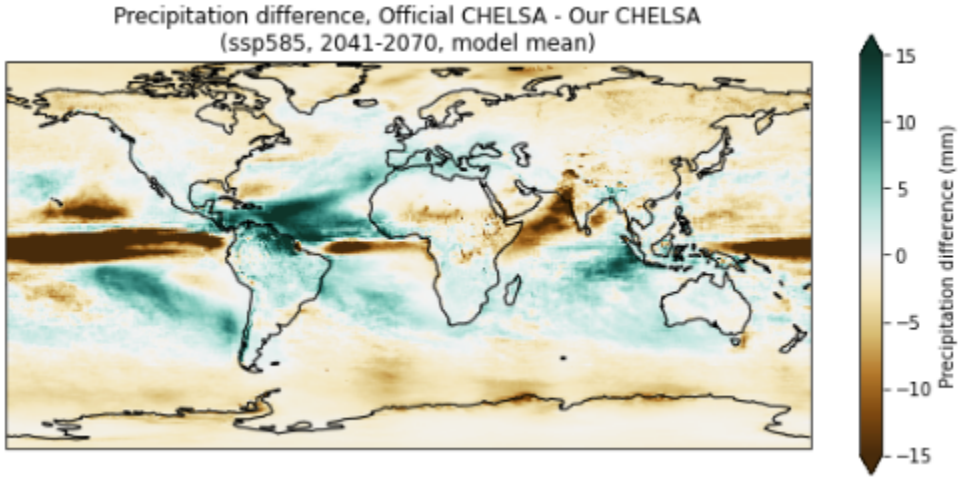

Figure 29. Difference in annual precipitation between CHELSA_BC and CHELSA_WW for 2041-2070, averaged across three models.

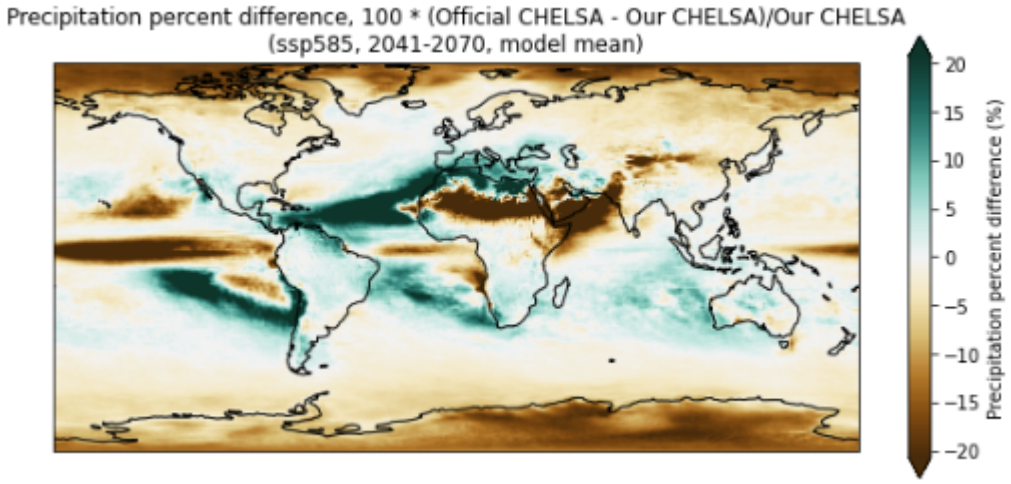

Figure 30. Percent difference in annual precipitation between CHELSA_BC and CHELSA_WW for 2041-2070, averaged across three models.

4.3.2.2 2071-2100

For the late 21st century period (Figures 31 and 32), differences in annual precipitation between CHELSA_BC and CHELSA_WW are somewhat stronger than in the mid-century period. Strong mixed sign differences continue in the equatorial ocean regions. Higher latitudes are consistently drier in CHELSA_BC than in CHELSA_WW. Unlike temperature, there was not a single model that contributed most of the differences; all models had similar magnitudes of contrast between CHELSA_BC and CHELSA_WW.

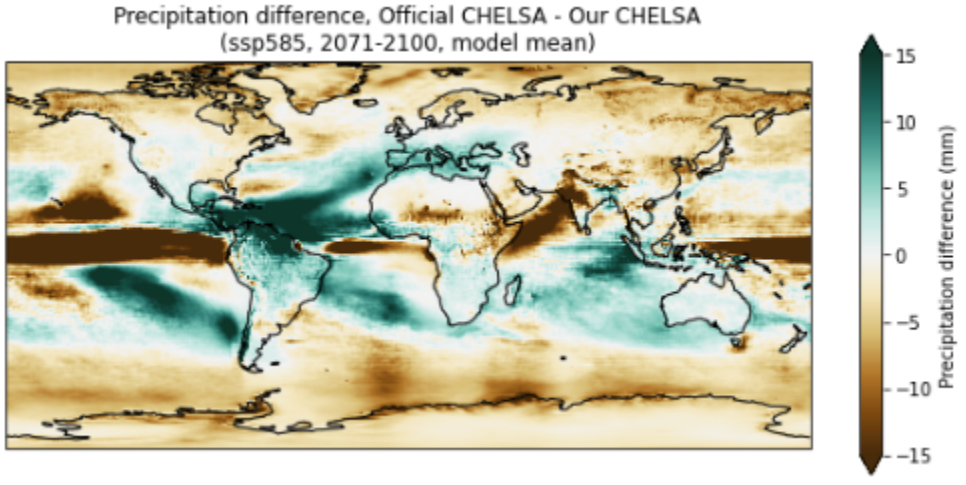

Figure 31. Difference in annual precipitation between CHELSA_BC and CHELSA_WW for 2071-2100, averaged across three models.

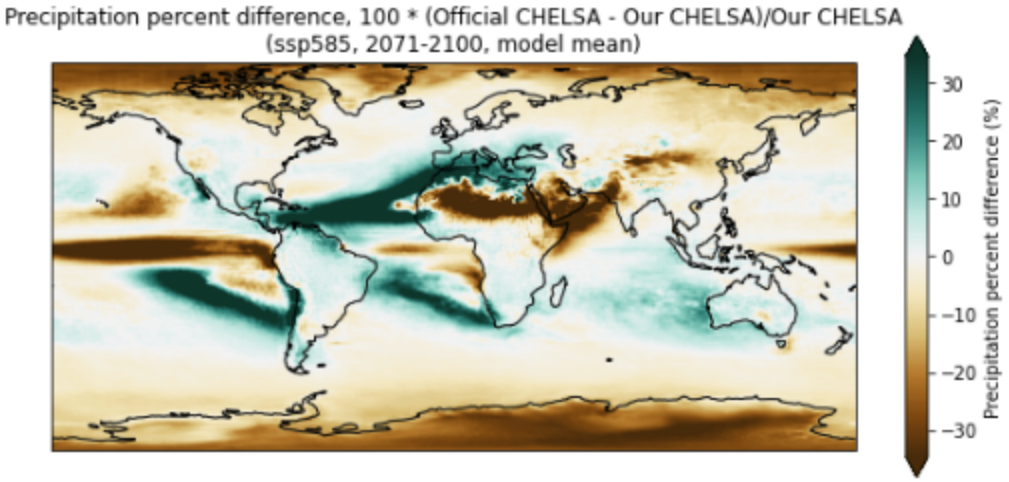

Figure 32. Percent difference in annual precipitation between CHELSA_BC and CHELSA_WW for 2071-2100, averaged across three models.

5. Code and Data Availability

Code for producing downscaled monthly climatologies for any model, ensemble member, scenario, time period and/or warming level is available at https://github.com/WoodwellRisk/CHELSA_downscaling.

We are in the process of posting the CHELSA_WW datasets to a public repository. In the meantime, the CHELSA_WW datasets are available upon request from the Woodwell Risk Team.

6. References

Karger, D.N., Conrad, O., Böhner, J., Kawohl, T., Kreft, H., Soria-Auza, R.W., Zimmermann, N.E., Linder, P., Kessler, M. (2017): Climatologies at high resolution for the Earth land surface areas. Scientific Data. 4 170122. https://doi.org/10.1038/sdata.2017.122

Lange, S.: Trend-preserving bias adjustment and statistical downscaling with ISIMIP3BASD (v1.0), Geosci. Model Dev., 12, 3055–3070, https://doi.org/10.5194/gmd-12-3055-2019, 2019.

Thornton, M.M., R. Shrestha, Y. Wei, P.E. Thornton, S-C. Kao, and B.E. Wilson. 2022. Daymet: Daily Surface Weather Data on a 1-km Grid for North America, Version 4 R1. ORNL DAAC, Oak Ridge, Tennessee, USA. https://doi.org/10.3334/ORNLDAAC/2129